Lally

TROPICAL WIND, ENERGY CONVERSION, AND REFERENCE LEVEL EXPERIMENT (TWERLE)

FINAL STATUS REPORT

For Period Ending 30 June 1976

TROPICAL WIND, ENERGY CONVERSION, AND REFERENCE LEVEL EXPERIMENT (TWERLE)

Status Report for Period Ending 30 June 1976

This is the final status report of the TWERLE program, as contract support from Goddard Space Flight Center terminated as of 30 June 1976.

A complete summary of all facets of the program will not be attempted in this report. This report consists of the flight status as of 30 June and four appendices, the most recent of which Dr. Paul Julian presented at the XIX COSPAR meeting on 10 June 1976. Dr. Julian condensed the TWERLE program in this paper and presented a concise summary of "first look" data.

On behalf of the Global Atmospheric Measurements Program group at NCAR we extend full acknowledgment to all participants in the TWERLE project and express our appreciation for being part of the TWERLE Team.

TWERLE STATUS AS OF DAY 182 (30 June 1976)

SITE	FLOWN	SHCD	NHCD	NOT HEARD	NATURAL DOWN	TOTAL DOWN
CHCH	139	0	10	3	94	105
ACCRA	50	4	32	2	12	50
ASC	115	15	47	3	50	115
SAMOA	107	12	31	1	63	107
TOTAL	411	31	120	9	219	377

34 balloons are flying

182 balloons down as of day 182

Average life of all TWERLE balloons - 66 days
Longest lifetime of those down is ID 1431 up for 307 days
Longest lifetime of those still up is ID 0315 up for 252 days

C.5.2 Application of the Data Collection System on Nimbus 6: The TWERL Experiment

Paul R. Julian, TWERLE Team Leader
National Center for Atmospheric Research*
Boulder, Colorado 80303

Abstract

The Tropical Wind, Energy Conversion, and Reference Level Experiment using the location and data collection system on Nimbus 6 is described. TWERLE made use of 411 instrumented balloon platforms launched July through September 1975 at three locations in the tropics and in October - February from Christchurch, New Zealand. The configuration of the system and its evaluation are described. Some scientific highlights including trajectory behavior and wave motions detected by the instrumented balloons are discussed.

* The National Center for Atmospheric Research is sponsored by the National Science Foundation.

C.5.2 Application of the Data Collection System on Nimbus 6:
The TWERL Experiment

Paul R. Julian, TWERLE Team Leader
National Center for Atmospheric Research
Boulder, Colorado 80303

1. Introduction

The Nimbus 6 spacecraft carries an experiment designed to locate and collect data from a large number of drifting platforms. In the case of the Tropical Wind Energy Conversion and Reference Level Experiment or TWERLE, these platforms were instrumented balloon platforms designed to float on a constant density surface.

The design, launching, and tracking of these balloon platforms represents the work of a large number of people, all of whom, while essential to the success of TWERLE, cannot be acknowledged individually here. The TWERLE is a joint program of the Goddard Space Flight Center, NASA, the University of Wisconsin, and the National Center for Atmospheric Research.

TWERLE is a GARP-related experiment. The location and data collection system on Nimbus 6 represents an effort, a successful effort, to fly a simple, reliable system which uses simple, low-cost platform expendables. The concept of a random Doppler system allowed simplicity and low cost with no sacrifice in position accuracy. The concept of an instrumented balloon platform allowed not only the determination of Reference (Level) Information for a global observing system, but has proven as well to allow the probing of various kinds of wave activity at balloon altitude.

2. The System

The TWERLE platforms consist of, apart from the non-extensible 3.5 m diameter balloon envelope, the necessary electronic, solar-cell array, and antenna to transmit 400 mHertz signals to the spacecraft once each minute. The transmissions of unknown frequency (within a 10 kHertz pass band) are self-timed based upon a nominal duty cycle and are not controlled by the space-craft equipment. In addition, each platform carries sensors to detect ambient temperature, pressure, and geometric altitude above the sea surface. Also, a geomagnetic field sensing device was incorporated into the balloon train which cut the platform down should it move north of 20° geomagnetic north. On the daylight portion of each orbit the space-borne equipment detects, demodulates, and stores the Doppler signal and sensor telemetry for platforms within range of the satellite. Processing of the Doppler signals on the ground provides the position and velocity of the platform.

It is important to note that the random Doppler system as used in TWERLE allows a solution to the full Doppler equation, but with an assumption as to the nature of the platform motion. Thus, for each coupled set of satellite passes, the equation is solved for two position and two velocity components plus a frequency bias for each pass: a total of six unknowns. The assumption is that the platform motion, between the first contact on pass A to the last on pass B, is unaccelerated great-circle motion. This solution <u>does not</u>, then, determine a position on pass A, and another on pass B, with the difference vector representing the velocity vector.

The flight level of the balloons was at a nominal (standard atmosphere) density level of 150 mb. Thus, in the tropics the flight level was in the upper troposphere while in mid- and high-latitudes it was in the lower stratosphere.

A total of 411 TWERLE balloons was launched: fifty from Accra, Ghana (5^{o}N, 0^{o}W), one hundred and fifteen from Ascension Island (8^{o}S, 14^{o}W), one hundred and seven from American Samoa (14^{o}S, 170^{o}W) and one hundred and thirty nine from Christchurch, New Zealand (44^{o}S, 173^{o}E). All three tropical sites commenced launching on 29 June and Ascension and Samoa completed the launch phase in late September - early October. The Accra site launched only 50 platforms and was closed early because of the high frequency of trajectories into the Northern Hemisphere. After launching some test flights in early June, the Christchurch site resumed launching in early October and continued through late January.

3. System Evaluation

The design parameters for the random Doppler system on Nimbus 6 were 5 km location and 1.5 mps velocity accuracy (both vector rms). The accuracy realized by the system has been found (not unexpectedly) to be a function of platform-satellite relative geometry and the actual trajectory of the platform over the two-hour interval involved in contact with the satellite. Ground-truth in the form of dozen FPS-16 radar tracks of TWERLE platforms during the interval in which the satellite was determining position and velocity indicates that the 1.5 mps vector rms accuracy is met when optimum geometry and well-behaved platform motion exists. Moreover, the software algorithm used to solve the Doppler equations is capable of giving quantitative information on the nature of the solution so that vector errors in excess of 1.5 mps may be anticipated. Position accuracy is, with accurate satellite ephemeris, better than 5 km (rms). Experimentation with the algorithm has shown that a definite improvement is realized if use is made of the oscillator bias history for estimating the initial Doppler curve inflection point.

The evaluation of the pressure, altitude, and temperature sensors is continuing. Experience to date indicates radio (geometric) altitude to an accuracy of a few meters with system precision of about 25 m (rms). Temperature accuracy is unknown but comparisons with radiosonde measurements indicate TWERLE temperatures average about 1^{o}C colder. The pressure accuracy is difficult to state because of lack of independent measurements at altitude and the detection in at least a portion of the sensors of a creep or drift over time. The sensitivity of the pressure sensor, however, was extremely good, on the order of 0.25 mb.

The launch strategy planned for TWERLE was based upon anticipated southward drift of the platforms, from the tropics where most of them were launched, into higher latitudes. This behavior was observed and introduces a complication in interpreting the statistics of mean lifetimes, since the vicissitudes of flying in the upper tropical troposphere are much greater than in the lower stratosphere of mid- and high-latitudes. Table 1 provides a summary by launch site of the disposition and mean lifetimes of the TWERLE platforms. In constructing this table some unresolvable causes of failure, electronic, balloon envelope, and weather-induced failure, are lumped into the 'natural' category. In summary, TWERLE achieved a level of 95 platforms up and working on 17 August and the number remained above that level, but did not exceed 125, until mid-February. As of 8 May, 37 platforms were still flying.

4. Some Scientific Highlights

The data analysis phase of TWERLE is just beginning and the full scientific content of the data is not yet known. Maps of the 150 mb wind field using TWERLE and conventional data, which have not yet been constructed, will provide the basic analysis material. The Reference (Level) Information experiment involving a meshing of the TWERLE-observed balloon and buoy reference information and the NCAR General Circulation Model is also not yet completed.

However, we have chosen some material which we believe illustrates some important scientific contributions to the understanding of the atmosphere which have been indicated by TWERLE. Figure 1 illustrates something of the coverage achieved by our platforms. On this Mercator projection of the globe we show the number of reports totalled over a 30-day period (mid-August to mid-September) in each five-degree longitude-latitude interval. During this period an average of 95 platforms launched from Ascension and Samoa were flying. The high concentration in the immediate vicinity of and immediately downstream of these launch sites is expected. In addition, a band of relative high report density can be seen at the latitude (~20°S) of the subtropical jet stream. Moreover, a large-scale 'concentration' of platforms occurred in the tropical Atlantic region and a virtual absence of reports can be noted in the vicinity of the monsoonal easterly flow over northern Africa, the Indian Ocean, and Indonesia. This comment leads naturally to Figure 2.

This figure shows the distribution of platforms in the region of the tropical Atlantic on 4 August 1975. The cluster in the Gulf of Guinea-Cameroon region consists of 17 platforms: eleven of these were launched from Ascension over the period of two weeks. Three were launched from Ghana over a period of two weeks, and three from Samoa, one more than one month previous. This tendency for platforms in the upper tropical troposphere to cluster represents quite different behavior from the dispersion observed of platforms launched in mid-latitudes, e.g., in the French EOLE experiment. Such behavior suggests mean divergence fields in space-time in the tropical upper troposphere occurring over dimensions of thousands of kilometers and days to weeks.

The basic trajectory data characteristic of the quasi-Lagrangian behavior of superpressure balloon platforms contains information on the behavior of the atmosphere which is quite valuable. We are, however, not comfortable with this type of information owing to its unconventional form and to the general intractability of the Lagrangian equations. Figure 3 is presented as an example of what information is contained in the trajectory data. Shown is a portion of the trajectories of two platforms launched the same day, 2 June, from Christchurch, N.Z. The trajectories cover the period from 30 June to 13 July. The two platforms remain quite close together -- less than 50 kilometers apart for the first four days -- so they cannot always be plotted separately. (During these days the largest vector wind difference observed between the platforms was 1.4 mps!) The tracks of the platforms were drawn using both the position and the velocity data. That is, if the average speed over a 24-hour period indicated that the distance covered was larger than the distance between the two locations the trajectory was adjusted to reflect that fact. We note that the cycloidal-type motion strongly indicated here is not unexpected on the anticyclonic-shear side of a jet stream in the presence of Rossby-type waves.

In Figure 4 we illustrate just one of the unexpected features of platform behavior. Of the 139 launches from Christchurch (44°S), eleven went into the Northern Hemisphere at some point in their lives. (This is as of 8 May.) Portions of the trajectories of nine of those platforms which illustrate movement northward out of mid-latitudes into the tropics are shown. There is obviously a preferred location for such a phenomenon to occur. Also notable is the fact that two of these platforms went into the Northern Hemisphere immediately from launch -- they were, however, launched on the same day.

The final illustrations provide evidence that the instrumented balloon platform is a powerful tool for investigating wave motion of various types in the free atmosphere. The University of Wisconsin colleagues have noted to date the following classes of wave motion: the neutral balloon oscillation with a period of 3 to 4 minutes; orographic lee waves with periods of 6-10 minutes; and, with special observational techniques and platforms, internal gravity waves with periods of 30-60 minutes. On launch day each platform was monitored until it passed over the radio horizon by recording the telemetry through a ground receiver. Not only did this procedure allow us to check the status of each platform as it went into altitude, it made available in many cases hours of data from the sensors. These data have been used to investigate wave activity revealed by the balloon motion. In Figure 5, the spectrum of ambient pressure measured once per minute over a period of about three hours is shown. The neutral balloon oscillation (NBO), caused by the continuous process of the balloon seeking its equilibrium density level in the face of all perturbing influences, has a predicated period of 3 to 4 minutes. The observed peak in the spectrum at 4 minutes is identified as the NBO. This particular platform arrived at altitude during relatively strong zonal flow over the mountains immediately upstream of Christchurch. The features at periods of 6 and 7.5 minutes on the spectrum are tentatively identified as signatures of lee (standing) waves associated with flow over the orographic barrier. Finally, the peaks at periods of 17 and 38 minutes are thought to be evidence of an internal gravity wave(s). We show in Figure 6 yet another kind of 'wave' phenomenon. In this figure the pressure, temperature, and radio altimeter data for consecutive passes for a platform located south of San Cristobel Island in the Solomon Islands. The ordinate scales are adjusted so that pressure and altitude are hydrostatically related and temperature is scaled to both of these by the dry adiabatic relationship. On the fifteen minutes of the first overpass the amplitude of balloon motion is typical of that usually seen.

On the second pass, the balloon undergoes a spectacular displacement, rising some 710 meters in 8 minutes. Note the consistency in all three variables -- pressure and altitude are beautifully hydrostatic and temperature vaies slightly greater than dry adiabatically. A visual check of the appropriate satellite photos indicates major convective activity in the area. From the behavior of the platform and its relatively strong horizontal velocity, we infer that it was moving directly over a rapidly developing convective cell. Complete analysis of the balloon equation of motion and the sensor data will enable us to measure accurately the vertical motion field experienced by the platform; a crude estimate here gives our motion on the order of 3.5 mps.

5. Conclusions

The TWERLE Team believes that the Experiment has made a number of significant technical

and scientific achievements. We have shown that a simple, low-cost location and data collection system is possible. Evaluation of that system has shown that it meets and even exceeds its design goals. We have learned a great deal about position and velocity determination from Doppler signals. We have shown that the instrumented superpressure balloon platform is a powerful tool for observing the atmosphere, including wave phenomena in the upper troposphere and lower stratosphere that are unobservable by other means. We have learned that the tropics behave differently than the higher latitudes in that large-scale quasi-persistent convergence fields affect the dispersion of drifting platforms. Qualitatively we have noted phenomena of these quasi-Lagrangian sensors that require quantitative explanation in terms of the mechanism of the general circulation.

And we have learned some lessons. We have learned, with others, that it is very difficult to build a fail-safe cut-down system. We knew that measuring atmosphere pressure to a fraction of a millibar at 150 mb is a challenge -- we proved that it is indeed.

One final fact is clear. We have not yet begun to extract the wealth of scientific information that is contained in our data.

6. Acknowledgements

The TWERLE Team: Charles Cote, GSFC (NASA); Verner Suomi, University of Wisconsin; Will Kellogg, Vincent Lally, and Paul Julian, NCAR, express their appreciation to the many colleagues who have made the program a successful one. We wish to dedicate this and future contributions to John Kruse and Charles Blair, who lost their lives in a tragic aircraft accident while traveling on TWERLE business.

Table 1

TWERLE Platform Statistics (as of 8 May 76)

Launch Site	# launched	Mean life (days)	Natural	Cutdown	SH Cutdown	Electronic	Alive
			(percent)				
Christchurch	139	87	61	6	0	8	25
American Samoa	107	66	46	29	11	14	0
Ascension	115	47	36	40	14	10	0
Accra	50	22	14	66	6	14	0
TOTAL	411	62	44	29	8	11	8

Figure Captions

Figure 1. Total number of reports from TWERLE balloon platforms from 13 August to 12 September in 5^{o} longitude-latitude squares. An average of 95 platforms were reporting in this interval.

Figure 2. Map of the tropical Atlantic region showing the location (only) of TWERLE balloons on 4 August 1975.

Figure 3. A portion of the trajectories of two TWERLE platforms over the eastern Pacific. The numbers below the locations indicate the date and above the height of the 150 mb surface in diameters from the sensors. If only one position and wind are shown the two platforms were too close to resolve on the map.

Figure 4. Portions of the trajectories of nine platforms launched from Christchurch, N.Z. illustrating the paths taken out of middle latitudes into the tropics. For each ID the launch date (first column), the approximate day the balloon entered the tropics (second column), and the day of death (last column) are shown.

Figure 5. Variance spectrum of pressure measured by TWERLE balloon at altitude on 8 December 1975. The spectrum was calculated from approximately three hours of telemetry with values measured once per minute.

Figure 6. Plot of the altitude, pressure, and temperature, from three successive passes of Nimbus 6 over ID 0103 located in the south Pacific, November 12/13, 1975. The passes are separated -- the time scale and the variable scales are shown.

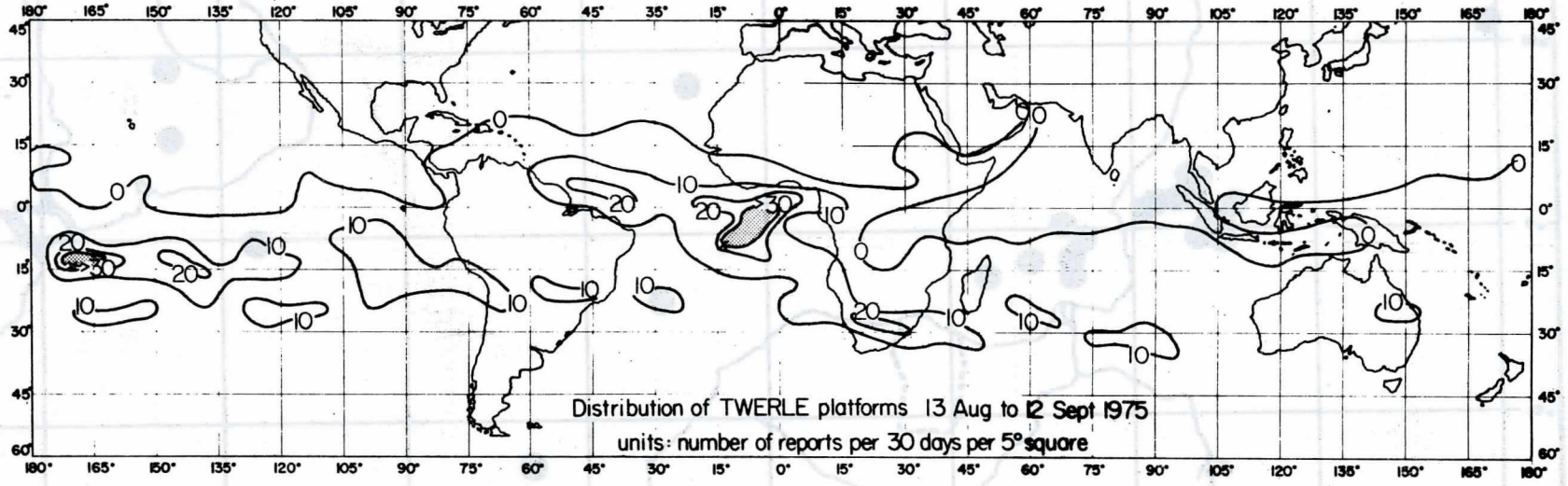
Distribution of TWERLE platforms 13 Aug to 12 Sept 1975
units: number of reports per 30 days per 5° square

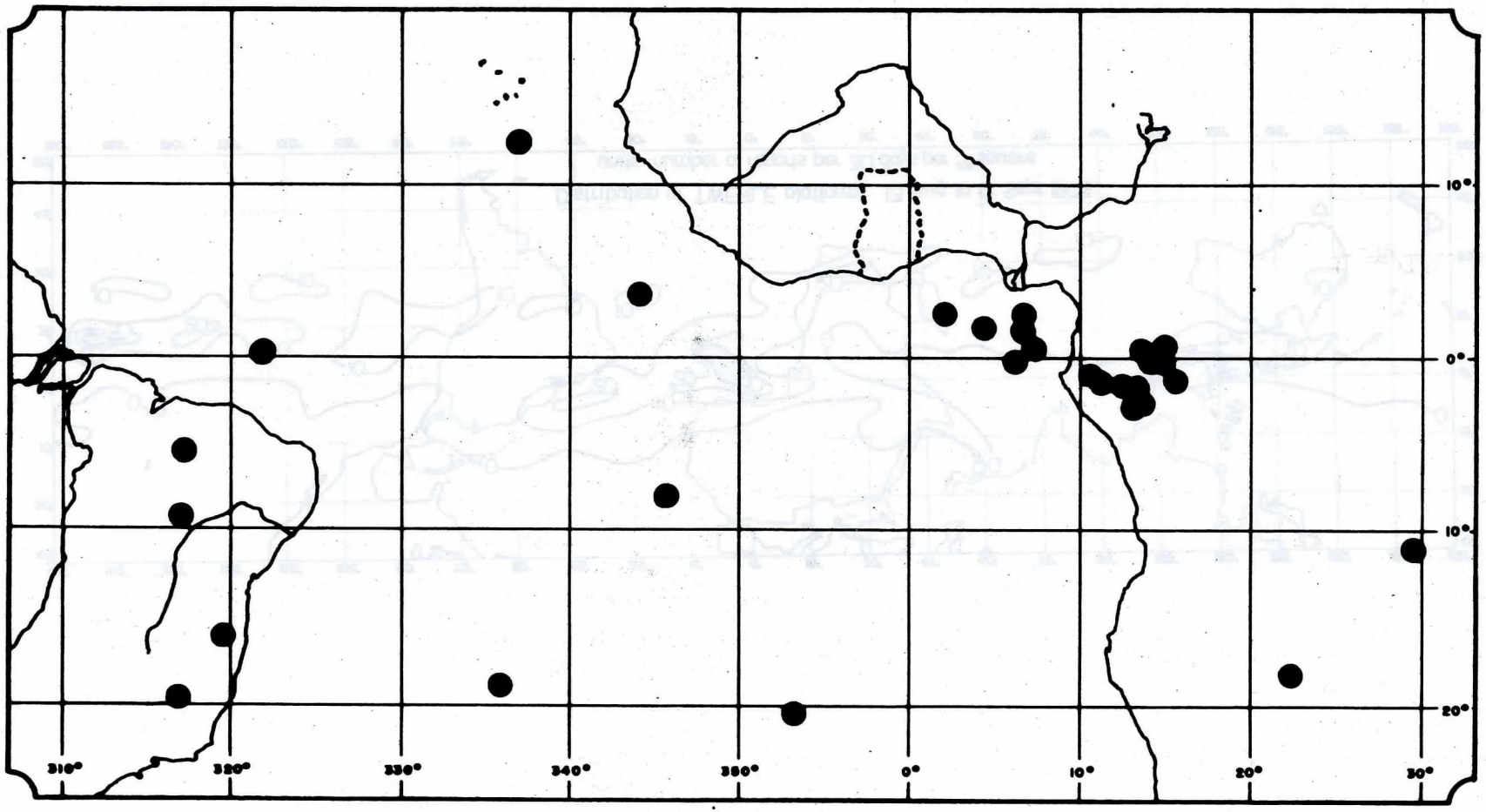

TWERLE
100 mb
122 4 August 1975

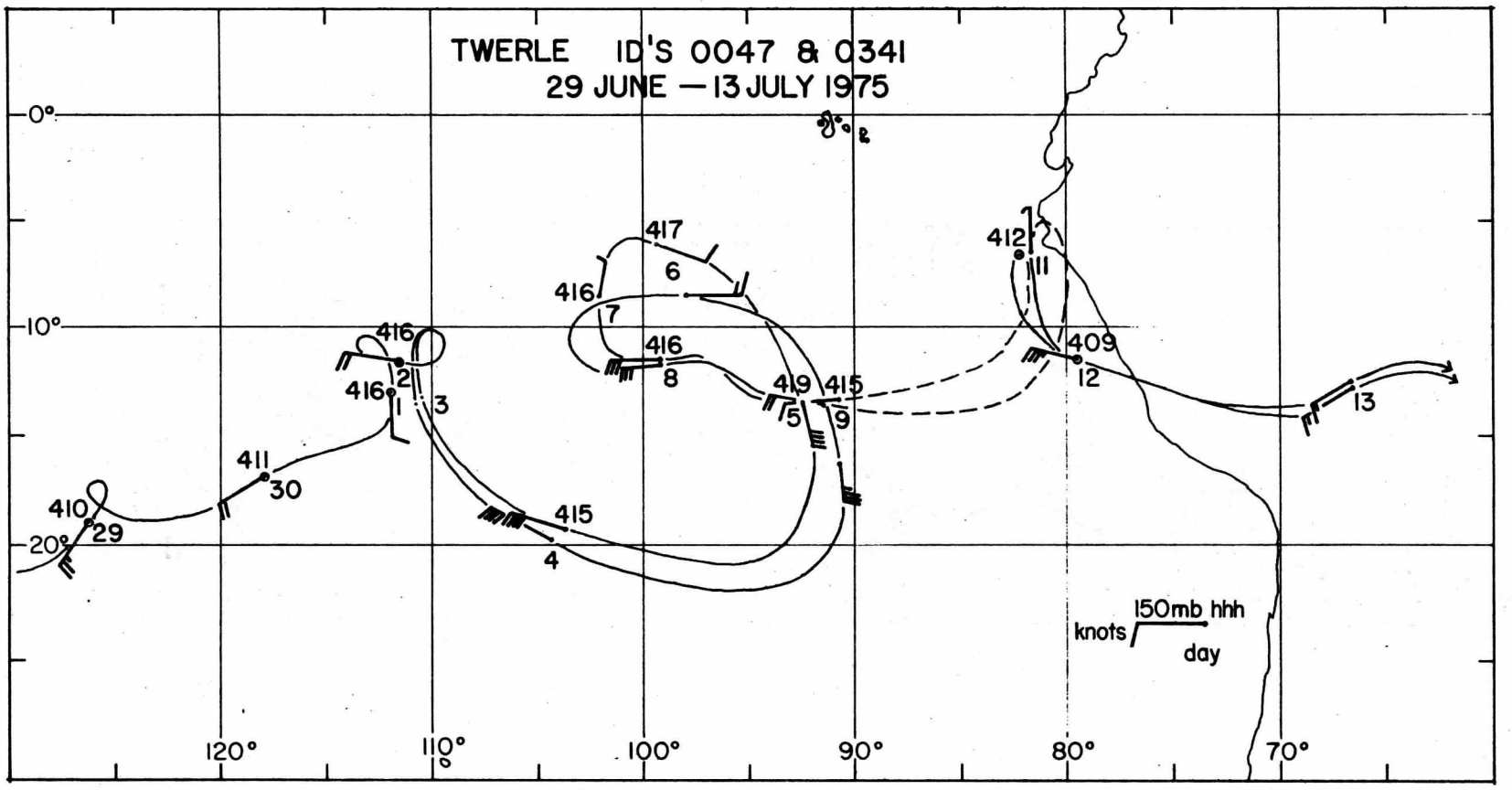
TWERLE ID'S 0047 & 0341
29 JUNE — 13 JULY 1975
0°
10°
20°
120°
110°
100°
90°
80°
70°
410
29
411
30
416
1
416
2
3
415
4
417
6
416
7
416
8
419
5
415
9
412
11
409
12
13
knots
150mb hhh
day

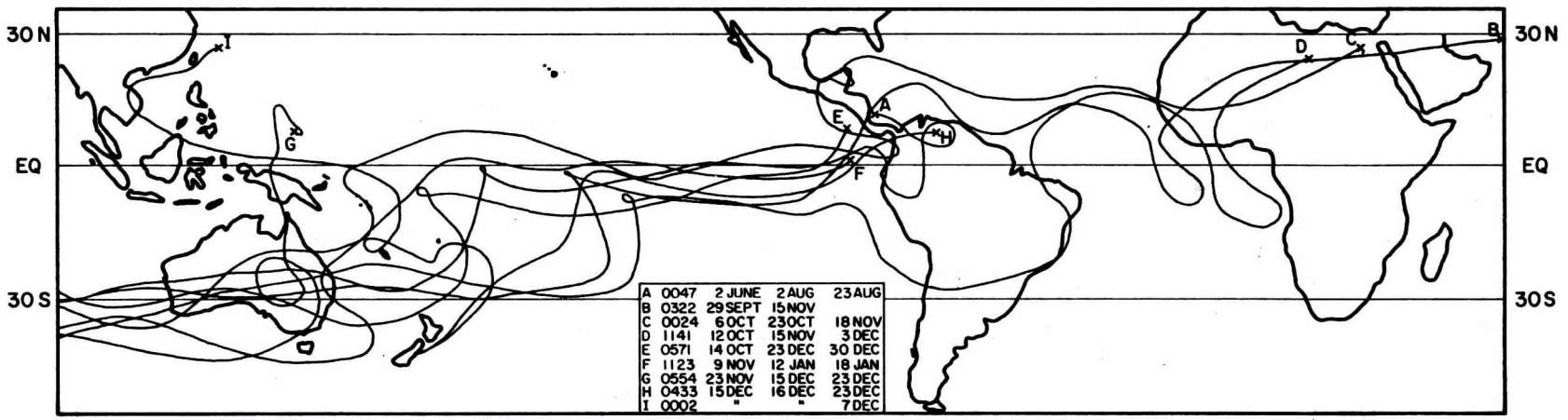
30 N
EQ
30 S
30 N
EQ
30 S
A 0047 2 JUNE 2 AUG 23 AUG
B 0322 29 SEPT 15 NOV
C 0024 6 OCT 23 OCT 18 NOV
D 1141 12 OCT 15 NOV 3 DEC
E 0571 14 OCT 23 DEC 30 DEC
F 1123 9 NOV 12 JAN 18 JAN
G 0554 23 NOV 15 DEC 23 DEC
H 0433 15 DEC 16 DEC 23 DEC
I 0002 " " 7 DEC

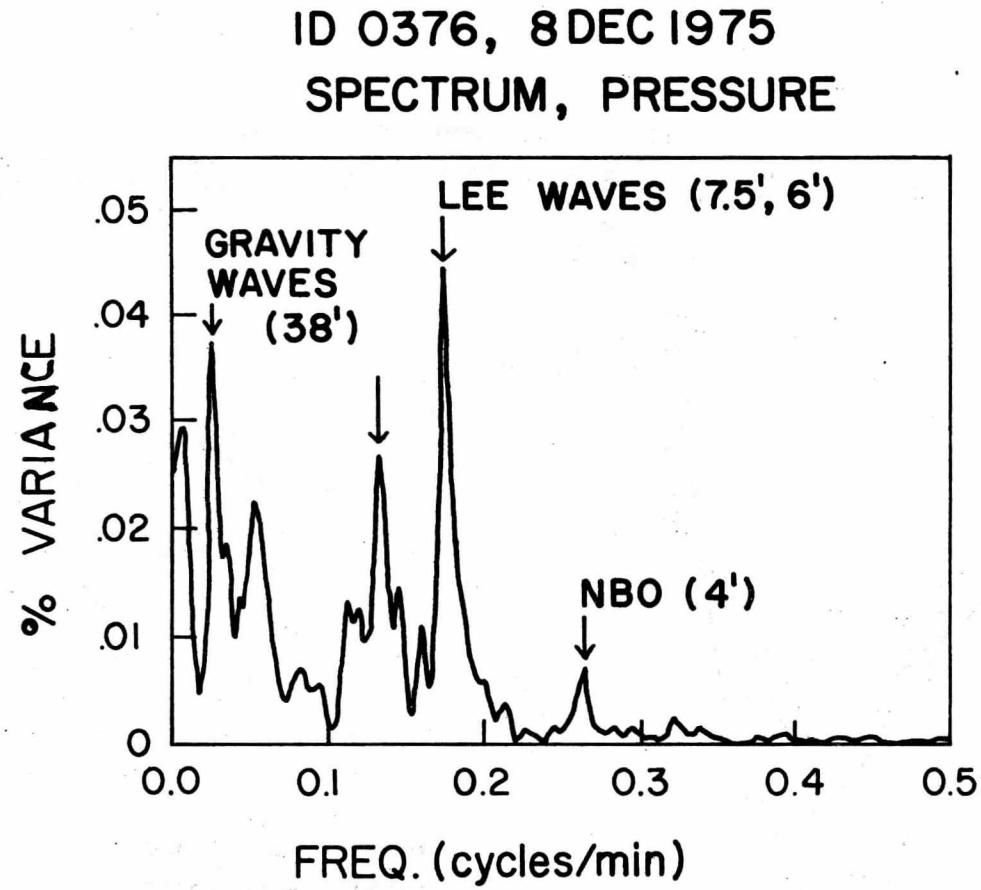
ID 0376, 8 DEC 1975
SPECTRUM, PRESSURE
LEE WAVES (7.5', 6')
GRAVITY WAVES (38')
NBO (4')
% VARIANCE
.05
.04
.03
.02
.01
0
0.0
0.1
0.2
0.3
0.4
0.5
FREQ. (cycles/min)

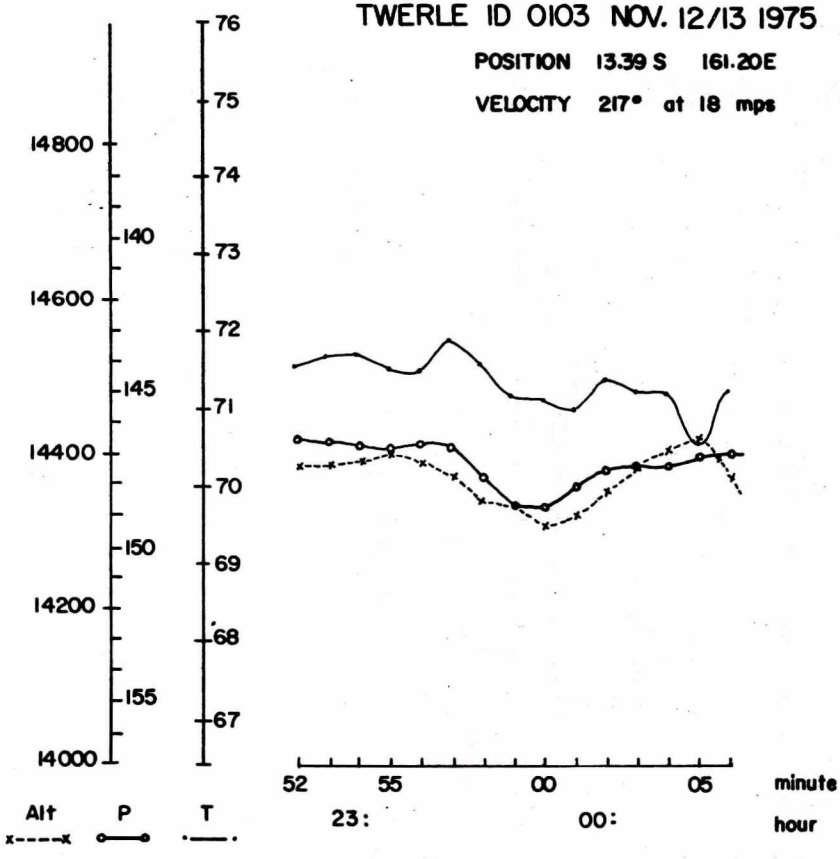
TWERLE ID 0103 NOV. 12/13 1975
POSITION 13.39 S 161.20E
VELOCITY 217° at 18 mps
14800
14600
14400
14200
14000
140
145
150
155
76
75
74
73
72
71
70
69
68
67
52
55
00
05
minute
23:
00:
hour
Alt
P
T

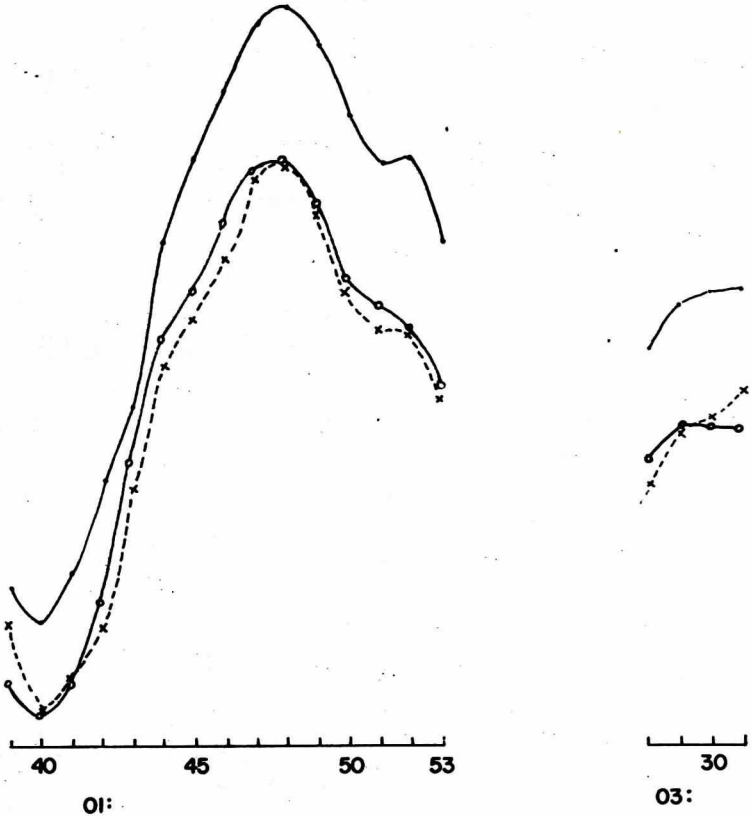
40
45
50
53
30
01:
03:

NATIONAL CENTER FOR ATMOSPHERIC RESEARCH
P. O. Box 3000 • Boulder, Colorado 80303
Telephone: (303) 494-5151 • TWX: 910-940-3245 • Telex: 45 694

22 January 1976

MEMO TO: TWERLE Team and Distribution

FROM: Paul Julian

SUBJECT: Analysis of the performance of the position-velocity algorithm

1.0 In my memo of 16 Oct. 1976 I mentioned that ground truth in the form of some FPS-16 radar tracks was available for about a dozen of the Ascension launches. The quantitative analysis of the simultaneous radar and Nimbus 6 RAMS tracks has been completed and will be reported on in Section 3.0. A dividend of the special gravity wave TWERLE platform flights was expected to be the availability of position and velocity data from 16 different IDs on the same balloon platform. The lengthy analysis that follows suggests to me that this dividend is unexpectedly large. I will argue that the analysis tells us or is capable of telling us a significant amount about the position/velocity algorithm and how it can be improved.

2.0 Analysis of the gravity-wave unit data. The special units designed and built at UWIS transmit serially 16 different IDs to the spacecraft. The one second transmissions are spaced approximately one second apart so that 16 doppler curves are received by the spacecraft with the maximum displacement in time being 37 seconds. We thus have a beautiful arrangement for testing the system precision. The GSFC software is unaware, of course, that the 16 doppler curves are from the same platforms and we have, thus, a sample of 16 different position and velocity determinations from the same population doppler curve.

I have selected eight cases for discussion here. These were chosen because of the range of performance of the system illustrated. In most cases data were from linked passes: that is doppler from 3,4, or 5 successive passes were employed to produce two-pass position/velocity data from 2,3, or 4 linked passes. This feature is especially valuable because it gives us information about the behavior of the algorithm when the platform undergoes a torturous or non-great-circle trajectory. The solution of the doppler equation which the algorithm employs, it will be recalled, is that the platform describes unaccelerated great circle motion during the time between first contact, first pass and last contact, second pass.

The eight cases selected are presented in the form of tables. Each table contains (besides day, time, etc.) frequency counts of the latitude and longitude determined and a sub-table showing the velocity components

stratified by the quality figure and the oscillator bias difference (in Hertz) found by the solution. In each case there are not always 16 two-pass solutions available: in some cases the solution was in the form of two single-pass cases (see my memo of 19 Nov. 1975). These latter solutions are not considered here.

Case 1. This case was selected because all 16 solutions had high quality figures (>40) and the dispersion of the positions and velocity components was comparatively small. This case is representative of the best system precision. The range of latitudes was .03 degrees (equal to about 3 km); the range of longitudes .05 degrees (5 km); and the range in velocity components was 0.9 mps. The sub-table showing the distribution of velocity components as a function of the quality figure, Q, and the difference in oscillator bias, ΔO, is especially instructive. Thirteen of the 16 solutions had $Q \geq 45$ and $\Delta O \leq 1$. The range in the east-west component U for these cases was 0.2 mps and north-south, V was 0.2 mps. The outliers in the velocity components are clearly associated with lower Qs and greater ΔOs. In this and succeeding tables the correspondence between the outliers in the velocity components and the associated positions is indicated by asterisk symbols. The not unexpected result is that the outliers in velocity correspond to the outliers in the positions.

Case 2. Here the quality figures are lower (all = 35). The same general conclusions as in Case 1 can be drawn.

Case 3. This is the first of a series of linked passes. On passes AB, the main velocity component outlier is associated with the largest ΔO and lowest Q. For those cases with $Q \geq 40$ and $\Delta O \leq 4$ the range in U is 0.8 mps and in V is 0.6 mps. For passes BC a more or less continuous variation in U and V as a 'function' of Q and ΔO is noticed. In general, this variation will be noted in all the cases with a few exceptions which will be explicitly acknowledged. A comparison of the two positions and the velocities in this and the remaining cases is deferred to Section 2.1.

Case 4. This case contains three linked passes from four consecutive orbits. Orbits AB shows still another example of the relationship between increasing Q, decreasing ΔO, and stabilizing velocity components. Orbits BC contain the first examples of a characteristic of the algorithm noted early in the TWERLE program and yet unexplained - the tendency for the solution to produce zero velocity components in a situation in which the balloon is obviously moving. Five of the 15 available cases have produced zero components, one with fairly high Q (=38) and a ΔO of zero. In the CD orbits we find a situation with very large ΔO (20 to 40 Hz) and associated impossible velocity components. A correlation here between Q and ΔO is quite obvious.

Case 5. Another four orbit combination showing two pass solutions with no correlation between Q and ΔO. In AB a consensus U & V seems to

be clear enough, but in the BC & CD orbits it is difficult to decide if the solutions are indicating any preferred velocities. The large variations, -11 to +12 mps, and 24 to 7 mps for U, e.g., with essentially the same Q and ΔOs indicate some problems with the algorithm. Analysis of the successive positions given in Section 2.1 suggest that a curved or convoluted trajectory is likely the cause of the difficulty.

Case 6. This case was chosen because the winds are apparently quite light and the trajectory somewhat uncertain. Again we note the relationship between the velocity outliers and low Q, high ΔO values, the large range of position and velocity component values, and a weak correlation between Q and ΔO. In orbits AB the solutions apparently become more stable in U & V with increasing Q (but note that the ΔO values are almost always >10 Hz). However, the solution with the highest Q and lowest ΔO has velocity components which do not agree with the others. The CD orbits here (only 7 available) are instructive, however, in the light of the comments to date.

Case 7. The inclusion of this case stems from the apparent well-behaved trajectory (next section) but completely puzzling group of solutions for the AB orbits. Note that the BC and CD orbits agree rather well on U and Vs which remain reasonably the same. However, there is no indication of any agreement in the AB solutions. From the data available here I can arrive at no explanation for such an occurrence.

Case 8. The only case with four linked-cases from five consecutive orbits. This is a good case for a summary because it includes many of the features exhibited in the other cases. I note a) for AB the solution with highest Q fails to determine a velocity, b) for the CD orbits only a single solution (of 16) is reasonable - it is the only one with $\Delta O < 16$. Why did this one succeed while the others failed? With the data at hand I can only guess, but it must involve a good determination of the inflection points on the two doppler curves. Only in one case were the guesses adequate, apparently. The same problem can be seen in the DE orbits. Two of the solutions are clearly way out, while the remaining 14 agree in excellent fashion.

2.1 Table 1 summarizes the 'best' or consensus position and velocity information for the cases with linked passes. The column headed 'great circle difference' is a velocity computed by differencing the positions and dividing by the time between successive orbits. For Case 5 and 6 a plot of the position and velocity data is appended. Perusal of the data in the Table reveals some items of interest, the significance of which is hard to describe since ground truth on the platform trajectories is completely lacking. Both cases 3 and 4 indicate wind vectors which are rotated counterclockwise from the great circle connecting the positions. However, in cases 7 and 8 this does not appear to be the case. In almost all cases the wind vector at the earlier two pass determination is nearer to the great circle direction connecting the positions.

Table 1. Linked pass summary. Consensus position/velocity data.

Case	Orbits	Lat	Long	U	V	ddd sss	great circle diff
3	AB	-38.38	267.66	37.2	-11.6	287/39.0	318/23.0
3	BC	-38.36	268.78	44.6	-8.3	280/45.4	
4	AB	-66.47	324.43	3.6	1.6	246/4.0	258/4.1
4	BC	-66.42	325.02	2.9	1.2	249/3.2	250/3.3
4	CD	-66.35	325.46	3.9	1.6	248/4.2	
5	AB	-64.29	58.44	11.5	-8.7	307/14.4	301/12.9
5	BC	-64.67	59.92	-8.1	-17.7	026/19.5?	015/18.4
5	CD	-65.69	59.28	23.7	-1.1	273/23.7?	
6	AB	-67.65	69.60	2.7	-0.4	278/2.8?	276/3.1
6	BC	-67.68	70.08	-1.2	1.1	132/1.6	195/2.0
6	CD	-67.56	70.16	3.4	3.2	226/4.7	
7	AB	???					
7	BC	-56.50	355.92	12.8	12.6	225/18.0	225/18.5
7	CD	-55.74	357.26	12.9	13.0	225/18.3	
8	AB	-65.89	318.95	2.1	-1.4	304/2.5	302/2.6
8	BC	-65.97	319.26	1.3	-2.2	329/2.6	319/3.0
8	CD	-66.10	319.54	3.1	-0.6	281/3.2	283/3.2
8	DE	-66.14	319.98	2.0	-0.9	294/2.2	

In view of the discussion in the previous section I note that the apparent trajectories in cases 3, 4, and 8 are reasonably well behaved with little or no curvature, whereas cases 5 and 6 are clearly confused trajectories. Case 7 is an enigma as orbits BC, CD indicate a well-behaved trajectory, but (as noted above) the solution for orbits AB seems hopeless. In general, the solutions for 3, 4 and 8 are more precise than those for 5 and 6, a result that might be expected. However, it is interesting that given enough sample Doppler curves from a platform undergoing a highly curved trajectory that some degree of precision is still apparently possible. System <u>accuracy</u>, however, in these cases is of course completely unknown.

2.2 From the cases shown here I draw the following conclusions:

1) In the happenstance of high quality figure (~40) and $\Delta 0$ less than about 10 Hz the probability is high that system <u>precision</u> is on the order of 5 km rms position and 1 mps velocity rms uncertainty.

2) The correlation between Q and ΔO is weak. There is independent information about the quality of the solution in the oscillator bias difference determined by the algorithm. This conclusion reinforces my views contained in the 19 Nov. 1975 memo. Clearly a good solution is dependent upon a good first guess of the doppler inflection points.

3) Occasional refusals of the algorithm to determine velocity components occur. It is not clear at all what causes such refusals and there is only a weak relationship of this behavior with Q and ΔO.

4) Some combination of Q and ΔO is a measure of system precision. Both position and velocity solution elements stabilize (are more precise) as Q increases and ΔO decreases.

5) Convoluted and non-great-circle trajectories of the platform influence the solution by a) affecting Q but b) for the same Q and ΔO a dispersion of position/velocity elements exists. Velocity components obtained by differencing successive two-pass solution positions are in reasonable agreement with the two-pass solution velocities themselves even in apparently rather tortorous trajectories. It is completely unknown, of course, how such positions and velocities correspond to the actual ones.

3.0 The FPS-16 radar track data represents the best source of ground truth for the position/velocity determinations. Radar track was performed on about 30 TWERLE Ascension launches but to get good ground truth only those tracks were used which spanned a portion of the 107 minutes between first contact with the platform and the subsequent orbit. In no case did the radar track span the entire 107 minutes. In reducing the radar data Cartesian geometry was employed and the entire record (position every 10 seconds) was not analyzed. Each track was checked for curvature by calculating the velocity components over sub-sections of the track.

The results are set out in Table 2. The time of first spacecraft contact with the platform is given; the TWERLE/RAMS position applies to this time. In a few cases the radar position has been adjusted (by using the velocities measured by the radar) to correspond to the first contact time. Six cases in which the radar track spanned a portion of the 107+ minutes between first and last spacecraft contact were available. The vector differences, TWERLE/RAMS minus radar track, are shown in the last column. The differences are on the order of 1 to 4 mps in magnitude for those cases occurring after early August. Before that time the algorithm was using data from the platforms with ranges in excess of 2500-3500 km; and, generally, this caused problems in the position/velocity algorithm. The 16 July and 4 Aug. cases have large vector errors, 33 and 13 mps in magnitude, and a recalculation of these with the revised algorithm might result in better agreement. However, I note that in both these cases the

Table 2. Ground truth - FPS-16 Radar track data, Ascension Island.

	Date	Id	S/c Contact GMT	Radar Track GMT	Q/ΔOsc	TWERLE/RAMS Pos Lat	TWERLE/RAMS Pos Lon	Radar Pos Lat	Radar Pos Lon	TWERLE/RAMS Velocity U	TWERLE/RAMS Velocity V	Radar Velocity U	Radar Velocity V	Vector diff T-R
199	18 July	1357	12:43	12:43-13:03	37/6	-8.80	343.73	-8.25	345.73	+33.1	+9.6	+1.4	-0.3	33.2 at 73°
216	4 Aug	1360	12:41	12:41-13:31	35/8	-8.24	344.53	-7.99	345.34	+20.6	-0.6	+8.4	-5.0	13.0 at 70°
227	15 Aug	0216	11:48	11:52*-12:37	35/15	-8.32	345.73	(-8.32	345.81)*	+15.6	-9.4	+15.0	-10.3	1.1 at 34°
231	19 Aug	1373	12:23	12:32*-13:36	40/13	-7.56	345.69	(-7.47	345.88)*	+5.6	+17.4	+2.5	+15.3	3.7 at 56°
247	4 Sept	1074	11:26	11:26-12:01	40/4	-8.08	345.21	-8.04	345.26	-2.1	-2.8	-4.0	-2.5	1.9 at 99°
254	11 Sept	0371	11:41	11:41-12:18	36/2	-8.04	345.81	-8.01	345.96	+16.4	-2.0	+15.4	-2.2	1.0 at 79°
	Cases with non-simultaneous track													
188	7 July	1464	11:58	10:21-10:54	38/2	-8.55	345.04	-	-	-10.3	-11.3	-13.1	-12.1	2.9 at 74°
190	9 July	0062	12:17	11:25-11:49	37/3	-8.21	345.07	-	-	-11.6	-3.9	-12.5	-4.2	0.95 at 72°
204	23 July	0173	12:38	11:07-11:40	37/9	-8.53	344.22	-	-	-15.4	-12.9	-19.2	-11.2	4.2 at 114°
206	25 July	1021	11:12	10:30-11:02*	34/31	-8.43	344.84	(-8.28	344.89)*	-0.9	-2.6	-16.7	-10.9	17.8 at 298°

quality figures are relatively high (35 and 37) and $\Delta\Omega$ relatively low (6 and 8 Hz), so it is not clear that better agreement with the radar data can be expected.

The direction of the vector difference shows a consistency over all cases which seems very significant. The directions range from 34 to 99 degrees with most of them in the range 70-80 degrees. This results from a consistent over estimate of the east-west component (and to a lesser degree the N-S component) by the TWERLE/RAMS algorithm relative to the radar. Since this direction (70-80°) is almost exactly in the cross-track direction at Ascension it suggests a systematic bias in the position/velocity algorithms. However, I have no idea as to what this bias might be ascribed to.

Table 3 indicates in crude form something as to the curvature of the balloon trajectories as tracked by the FPS-16. Each radar track was divided in half and the velocity components computed for each. The most pronounced curvature seems to have occurred for the 15 and 19 Aug. flights. In these cases, however, the vector differences are relatively small. There is no indication that the large vector differences on 18 July and 4 Aug. can be ascribed to an accelerated platform trajectory.

Table 3. Curvature estimates for trajectories

		Radar track velocities - mps	
18 July	1st half	1.7	-0.3
	2nd half	1.1	-0.4
4 Aug	1st half	8.2	-5.0
	2nd half	8.5	-5.0
15 Aug	1st half	15.8	-10.6
	2nd half	14.5	-9.9
19 Aug	1st half	1.9	14.2
	2nd half	3.2	16.5
4 Sept	1st half	-3.9	-2.7
	2nd half	-4.1	-2.3
11 Sept	1st half	15.5	-2.5
	2nd half	15.4	-1.8

4.0 As a result of this study of the accuracy and precision of the TWERLE/RAMS algorithm, I can conclude the following: more study of the interplay between the algorithm's quality figure and oscillator bias difference, and platform trajectory and platform-spacecraft geometry is needed. Additional ground truth in the form of platforms moving with known trajectories would be advisable. Some experimentation with the use of oscillator bias information in the algorithm is already underway - this is also necessary. The system has been proven to be a good system for platform tracking but I believe it can be made a better system with some moderate effort.

Case No. 1 Quality figures > 40, 25 contacts used in all cases.

ID GW 0157 Day 362

AB orbits Hour 1542 ± 1 #IDs available 16

Latitude	No.	Longitude	No.
−37.63	2	296.05	3
−37.64	4 (*) (**)	296.06	3
−37.65	5	296.07	4
−37.66	5	296.08	1
		296.09	2 (**)
		296.10	3 (*)

	U-wind	V-wind	Qual. figure	ΔOsc bias	#
*	17.9	18.2	41	18	
**	18.5	18.0	42	8	
	18.8	17.5	42	6	
	18.5-18.7	17.6-17.8	45-46	0-1	13

BC orbits Hour #IDs available

Latitude	No.	Longitude	No.

Case No. 2 Quality figures all 35, 25 contacts used all determinations

ID GW 0757 Day 005

AB orbits Latitude	Hour No.	0818 ± 1	#IDs available Longitude	14 No.
-22.00	14		42.15	3
			42.16	7
			42.17	4

U-wind	V-wind	Qual. figure	ΔOsc bias	
10.5	−0.4	35	9	
10.1	−0.6	35	7	
10.4	−0.3	35	7	2
10.4	−0.4	35	9	2
10.4	−0.5	35	9	
10.3	−0.3	35	9	
10.2	−0.3	35	8	
10.3	−0.4	35	8	2
10.3	−0.3	35	8	2
10.1	−0.4	35	5	

BC orbits Latitude	Hour No.	#IDs available Longitude	No.

Case No. 3 Quality figures > 38, 24-25. contacts used

ID GW 0757 Day 361

AB orbits Hour 1627 ± 1 #IDs available 8

Latitude	No.		Longitude	No.	
-38.36	1		267.63	1	
-38.37	3		267.64	1	
-38.38	3	(*)	267.65	2	
-38.39	1		267.66	1	
			267.67	1	
			267.69	2	(*)

	U-wind	V-wind	Qual. figure	ΔOsc bias
*	33.8	-11.2	39	10
	35.1	-12.6	39	2
	37.6	-11.5	40	4
	36.8	-12.1	40	3
	36.9	-11.9	40	2
	37.2	-11.5	40	2
	37.2	-11.6	41	4
	36.4	-11.6	41	3

BC orbits Hour 1812 ± 2 #IDs available 8 (17-23 contacts)

Latitude	No.		Longitude	No.	
-38.97	1	*	268.27	1	**
-38.98	1		268.72	1	
-39.00	1		268.77	1	
-39.05	1		268.78	1	
-39.36	1		270.27	1	
-39.39	1		270.37	1	
-39.41	1		270.46	1	
-39.45	1	**	270.50	1	*

Case No. 3 (cont)

	U-wind	V-wind	Qual. figure	ΔOsc bias	n
*	24.1	-16.2	38	13	21
	24.6	-15.4	38	5	19
**	51.8	-6.7	38	1	20
	26.6	-15.1	39	9	23
	24.3	-15.9	39	7	21
	44.9	-7.3	39	3	18
	44.6	-8.5	41	3	17
	44.8	-8.2	42	3	20

CD orbits	Hour	#IDs available
Latitude	No.	Longitude No.

U-wind	V-wind	Qual. figure	ΔOsc bias

Case No. 4 Variable quality figures, 25 contacts all determinations

ID GW 0760 Day 361

AB orbits Hour 10:55 #IDs available 15

Latitude	No.		Longitude	No.	
-66.46	2		324.34	1	**
-66.47	7	(*)	324.38	1	*
-66.48	5		324.43	6	
-66.49	1	**	324.44	1	
			324.45	2	
			324.46	4	

	U-wind	V-wind	Qual. figure	ΔOsc bias
*	0.1	-0.1	36	15
	3.8	0.7	36	5
**	4.4	1.1	36	1
	3.4	0.6	37	7
	3.8	0.8	37	6
	3.3	1.9	37	5
	3.7	0.9	37	4
	3.4	1.7	37	4
	3.6	1.5	37	4
	3.7	0.9	37	3
	3.9	0.1	37	3
	3.6-3.7	0.9-1.4	37	2-0

BC orbits Hour 12:42 #IDs available 15

Latitude	No.	Longitude	No.
-66.41	3	325.00	7
-66.42	12	325.01	8

U-wind		V-wind	Qual. figure	ΔOsc bias	#
0.0	?	0.0	37	2	2
0.0	?	0.0	38	2	
2.9		1.4	38	2	
3.1		1.4	38	2	2
3.0		1.2	38	1	3
3.2		1.2	38	1	
3.1		1.2	38	0	2
0.0	?	0.0	38	0	
3.1		1.1	39	1	2

CD orbits Hour 14 29 #IDs available 15

Latitude	No.	Longitude	No.
-60.66	1 *	325.05	1 Δ
-65.99	1 Δ	325.07	1 **
-66.01	1 **	325.32	1 *
-66.34	2	325.43-44	3
-66.35	9	325.45-46	5
-66.43	1	325.47	1
		325.51	1
		325.58	1
		325.53	1

	U-wind		V-wind	Qual. figure	ΔOsc bias
*	-52		-18	25	44
Δ	-97		-81	31	12
**	-96		-80	31	20
	0	?	0	36	8
	0	?	0	36	7
	+0.7		-0.2	39	11
	1.1		-0.1	40	13
	1.2		+0.1	40	13
	1.2		0.0	40	11
	3.9		1.7	40	8
	4.0		1.6	40	7
	3.9		1.6	40	6
	3.9		1.6	41	8
	4.2		1.7	41	6
	3.9		1.6	43	8

Case No. 5 Variable quality figures, less than 20 contacts used

ID GW 0760 Day 001

AB orbits Hour 05:41 #IDs available 16

Latitude	No.		Longitude	No.	
-64.26	1	*	58.38	1	*
-64.28	1	**	58.41	1	**
-64.29	5		58.42	2	
-64.30	7		58.43	2	
-64.31	2		58.44	6	
			58.45	3	
			58.47	1	

	U-wind	V-wind	Qual. figure	ΔOsc bias	#
	0 ?	0	27	6	
*	11.8	-9.4	30	14	
**	10.7	-8.3	30	10	
	11.7	-9.0	30	6	2
	11.5	-8.9	30	4	
	10.9	-8.2	30	3	
	11.4	-8.5	30	3	2
	11.5	-8.7	30	3	2
	11.6	-8.8	30	2	2
	11.4	-8.7	30	2	2
	11.2	-8.6	30	2	

BC orbits Hour 07:29 #IDs available 8

Latitude	No.		Longitude	No.	
-64.76	4		59.90	1	
-64.79	3		59.91	1	
-64.80	1	*	59.92	2	
			60.00	1	
			60.01	1	
			60.02	1	
			60.16	1	*

	U-wind	V-wind	Qual. figure	ΔOsc bias
	12.4	-7.0	30	9
	10.2	-8.1	31	9
	-11.4	-19.5	32	13
	-8.9	-18.1	32	9
	12.1	-7.1	32	8
	-8.6	-18.0	32	7
	-7.6	-17.3	32	7
*	-10.6	-18.6	34	15

CD orbits Hour 09:16 #IDs available 11

Latitude	No.		Longitude	No.	
-65.20	1	*	58.64	1	**
-65.22	1		58.70	1	
-65.24	1	Δ	58.82	2	
-65.66	1	ΔΔ	58.83	1	
-65.69	1		59.05	1	
-65.74	1		59.28	1	
-65.77	1		59.65	1	ΔΔ
-65.79	2		60.02	1	
-65.82	2	**	61.48	1	Δ
			61.70	1	*

	U-wind	V-wind	Qual. figure	ΔOsc bias
	0 ?	0	28	10
*	0 ?	0	29	45
**	27.4	-0.8	29	12
	25.1	-0.6	29	9
	27.4	+0.6	29	7
	28.4	+ 1.1	30	7
	23.7	- 1.1	30	2
	26.4	-0.1	31	12
Δ	7.6	-7.5	32	12
	6.6	-9.7	32	11
ΔΔ	7.0	-8.6	32	38

Case No. 6 Light winds, confused trajectory

ID GW 0760 Day 002

AB orbits Hour 0457 #IDs available 12

Latitude	No.		Longitude	No.	
-67.62	1		69.56	1	
-67.64	1	Δ	69.57	1	Δ
-67.65	4		69.59	1	
-67.66	3		69.60	2	
-67.67	1		69.61	2	
-67.68	1	**	69.63	1	
-67.79	1	*	69.65	1	
			69.66	1	
			69.75	1	*
			69.81	1	**

	U-wind		V-wind	Qual. figure	ΔOsc bias	#
	0	?	0	38	11	
Δ	+3.1		-1.0	39	25	
*	+2.1		+1.9	39	16	
	+2.7		-0.4	39	5	
	+3.0		-0.8	40	21	
	+2.9		-0.6	40	20	
	+2.8		-0.6	40	19	2
	+2.8		-0.8	41	18	
	+2.6		-0.5	41	16	
	+2.3		-0.9	42	13	
**	+0.6		+0.1	43	2	

BC orbits Hour 0644 #IDs available 8

Latitude	No.	Longitude	No.
-67.64	1	69.99	1
-67.68	6	70.07	1
-67.69	1	70.08	4
		70.09	1
		70.12	1

	U-wind	V-wind	Qual. figure	ΔOsc bias
*	−0.9	+0.4	39	19
	-0.4	+1.6	41	3
	+1.4	+2.7	41	2
	+0.6	+2.1	41	1
	0	+1.5	41	2
	+0.1	+1.9	42	1
	-1.2	+1.1	43	3
	-1.1	+1.1	43	3

CD orbits Hour 0835 #IDs available 7

Latitude	No.		Longitude	No.	
(-114)	1	*	(78)	1	*
-66.41	1	**	69.84	1	
-66.74	1	Δ	70.09	1	
-67.55	1		70.16	1	
-67.56	1		70.19	1	
-67.58	1		75.49	1	Δ
-67.63	1		75.56	1	**

	U-wind	V-wind	Qual. figure	ΔOsc bias
*	43	54	26	9
**	-35	-20	33	37
Δ	-33	-18	34	38
	-2.8	4.3	34	4
	-0.6	0.2	41	15
	4.0	3.8	41	6
	3.4	3.2	42	2

Case No. 7 Puzzling linked passes.

ID GW 0760 Day 363

AB orbits Hour 11:20 #IDs available 12

Latitude	No.	Longitude	No.
-56.95	1	353.53	1
-56.96	2	353.78	1
-56.97	1	354.17	1
-56.99	1	354.27	1
-57.04	2	354.29	1
-57.06	2	354.31	1
-57.13	1	354.34	1
-57.16	1	354.35	1
-57.17	1	354.36	3
		354.41	1

U-wind	V-wind	Qual. figure	ΔOsc bias
-27	-8	27	12
-27	-9	27	6
-24	-8	28	12
-26	-8	28	9
-14	-1	30	6
-23	-6	31	7
-3.4	0.3	32	23
-6.1	0.5	32	6
17	12	33	0
0 ?	0	34	19
-0.4	2.4	35	14
4	5	35	15

BC orbits Hour 13:04 #IDs available 8

Latitude	No.	Longitude	No.
-55.79	1 *	355.90	1
-56.34	1 **	355.92	2
-56.44	1 Δ	355.93	1
-56.49	1	355.98	1
-56.50	3	356.19	1 Δ
-56.56	1	356.48	1 **
		358.21	1 *

	U-wind	V-wind	Qual. figure	ΔOsc bias	#
*	9.9	-8.8	24	88	
**	1.6	3.9	33	7	
Δ	6.5	9.0	36	2	
	12.9	12.8	37	5	2
	12.6	12.6	37	4	
	13.0	12.7	37	4	
	12.1	12.4	38	5	

CD orbits Hour 14:54 #IDs available 16

Latitude	No.		Longitude	No.	
-55.73	1		357.25	7	(*)
-55.74	9		357.26	6	
-55.75	5		357.27	3	
-55.76	1	*			

U-wind	V-wind	Qual. figure	ΔOsc bias	
10.8	14.6	35	1	
12.9	13.1	36	2	
13.0	13.5	36	1	
12.5	14.1	37	12	
12.6	14.1	37	11	
12.6	13.8	37	9	
12.6	13.8	37	8	
13.6	12.8	37	7	
12.7	13.8	37	7	
12.7	13.6	37	6	
12.8	13.4	37	3	2
12.8	13.4	37	2	
12.8	12.9	37	1	
13.0	13.4	37	1	
* 10.9	14.8	38	44	

Case No. 8 Five linked orbits !

ID GW 0760 Day 360

AB orbits Hour 11:38 #IDs available 16

Latitude	No.	Longitude	No.
-65.86	1	318.95	6
-65.88	3	318.96	1
-65.89	11	318.97	3
-65.91	1 *	318.98	5
		319.04	1 *

U-wind	V-wind	Qual. figure	ΔOsc bias
2.2	-1.2	35	5
2.4	-1.2	35	5
2.4	-0.8	35	4
1.8	-2.1	36	10
2.0	-1.5	36	5
2.1	-1.6	36	5
1.9	-1.7	36	5
2.1	-1.6	36	4
2.2	-1.6	36	4
1.9	-1.8	36	3
2.1	-1.4	36	3
1.7	-1.1	36	3
2.2	-1.4	36	2
1.3	-2.1	37	7
1.4	-2.0	37	5
* 0 ?	0	38	5

BC orbits Hour 13:27 #IDs available 16

Latitude	No.	Longitude	No.
-65.97	8	319.25	3
-65.98	7	319.26	8
-66.00	1 *	319.27	4
		319.35	1 *

	U-wind		V-wind	Qual. figure	ΔOsc bias	#
←	0.8		−0.1	34	12	
	0	?	0	34	2	2
	0	?	0	34	0-1	2
	1.9		−1.9	35	2	
	1.9		−1.8	35	0	
	2.5		−0.9	35	0	
	1.9		−1.9	36	2	2
	1.8		−1.8	36	1	
	1.8		−2.0	36	1	
	1.8		−1.9	36	0	
	1.6		−2.2	37	1	
	1.3		−2.2	37	1	
	1.1		−2.2	37	1	

CD orbits Hour 15:14 #IDs available 16

Latitude	No.		Longitude	No.	
−62.63	14		337.38	14	
−65.82	1	**	318.30	1	**
−66.10	1	*	319.54	1	*

	U-wind	V-wind	Qual. figure	ΔOsc bias	#	
	−122	−91	27	34	2	
	−121	−89	27	32		
	−120	−88	27	31		
	−121	−88	27	28	2	
	−120	−88	27	21		
	−120	−89	27	20		
	−120	−88	27	17	2	
	−120	−88	27	16		
	−120	−88	28	21	2	
	−120	−89	28	19		
**	−127	−120	33	28		} two fewer contacts than the others
*	3.1	−0.6	40	0		

Case 8 (cont)

DE

orbits Latitude	Hour No.		#IDs available Longitude	16 No.	
-66.13	3		319.97	5	
-66.14	10		319.98	7	
< -71°	3	*	319.99	1	
			~290	3	*

	U-wind	V-wind	Qual. figure	ΔOsc bias	#
*	-118	-74	27	122	2
*	-118	-73	27	120	
	2.1	-1.2	39	3	
	2.1	-0.8	39	3	
	2.2	-0.8	39	2	
	2.1	-0.9	39	1	
	2.1	-1.1	39	1	2
	2.1	-1.1	39	0	
	2.4	-0.2	39	1	
	1.9	-0.9	40	2	
	2.1	-0.9	40	1	
	2.0	-0.8	40	1	
	2.1	-1.0	40	0	
	1.9	-0.8	41	2	

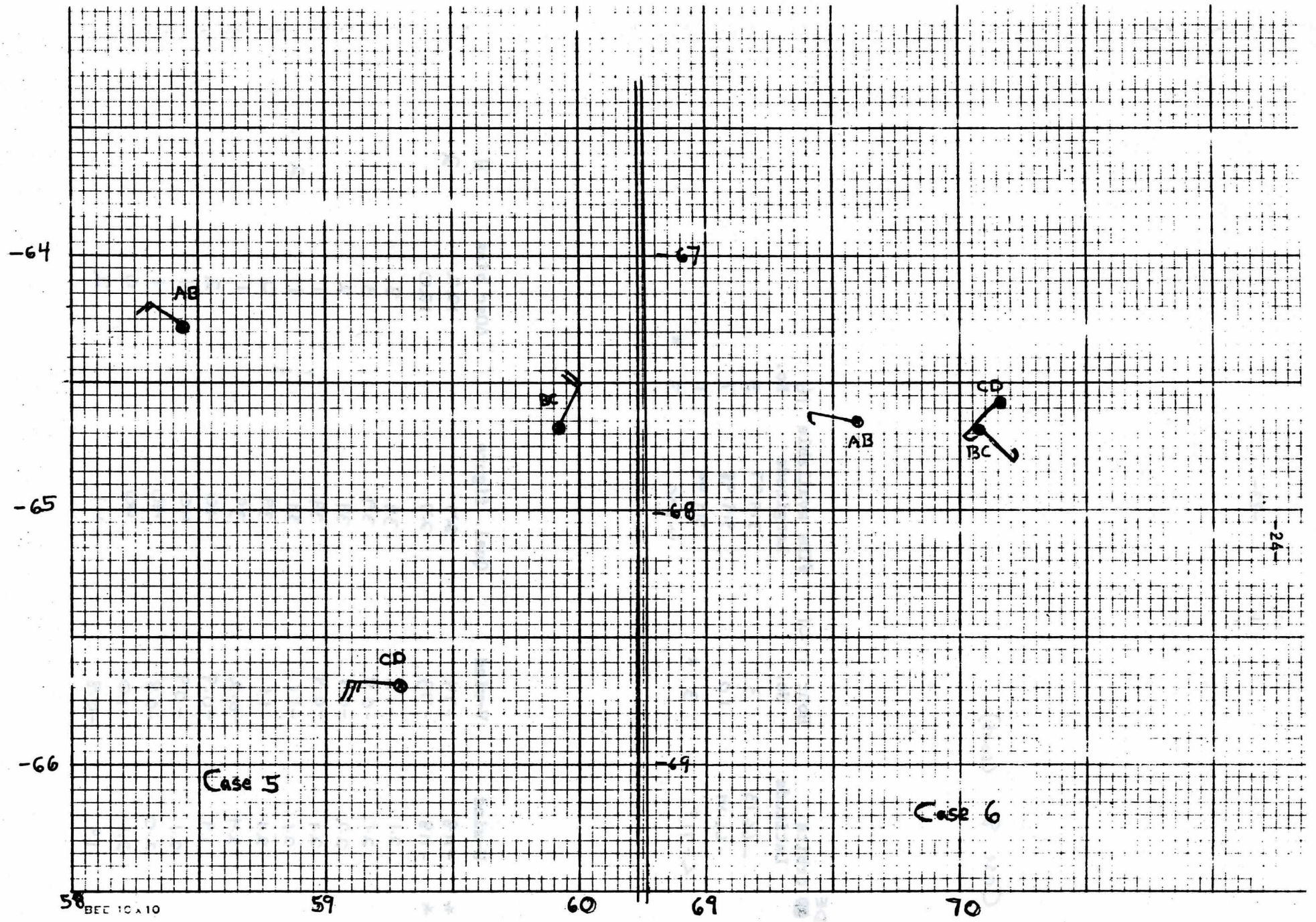
-64
-65
-66
-67
-68
-69
AB
BC
CD
AB
CD
BC
Case 5
Case 6
58
59
60
69
70
-24-

November 19, 1975

MEMORANDUM

TO: TWERLE Team and distribution

FROM: P. Julian

SUBJ: Evaluation of position/velocity algorithm

1.0 Introduction

1.1 This memo is prompted by an examination of the single- and two-pass solution results on the moving TWERLE platforms and upon empirical evidence concerning the day-to-day stability of the combined platform-spacecraft oscillator biases. In addition, we will comment on the changes instituted by Nimbus Operations in early August in which i) Doppler from estimated ranges, s/c to platform, in excess of 3000 km is eliminated from the Doppler set used in the algorithm and ii) two-pass cases in which the quality figure is less than 25 are reworked as two single-pass cases.

1.2 The following evaluation suggests to us that the position and velocity algorithm presently in use be modified to take advantage of the potential information available on oscillator bias. A suggested procedure for accomplishing this is set forth. Moreover, we conclude that treating poor two-pass cases as two one-pass cases leads to appreciably better results.

2.0 Results of investigation of oscillator biases

2.1 The oscillators on the TWERLE platforms and on the RAMS aboard the spacecraft result in the received Doppler offset from the nominal frequency. Since in our system there is no method of measuring directly the transmitted frequency, the position-velocity algorithm solves for the combined frequency bias. In the two-pass case, two biases are obtained one applying to each pass. In the single pass case, one bias applies to the position solution on one side of the spacecraft and the other on the ambiguous side. Early in the program we noticed that there was a relationship between the quality figure assigned to the two-pass case and the <u>difference</u> between the estimated oscillator biases. If the bias difference were large, greater than 100 hertz or so, then the quality figures were largely below 30 (many below 25). If the bias difference were small, less than 10 hertz, no cases were encountered with quality figures less

than 25. The explanation for this relationship seems obvious. Since the oscillator bias is the received Doppler at the inflection point of the Doppler curve (when the s/c is abeam the platform) and since the stability of the oscillators is such that we should not expect drifts of more than 20-30 hertz between passes, the similarity of the estimated biases on successive passes can serve as a good indicator of the stability of the solution.

2.2 Subsequent examination indicated that for a given platform oscillator biases estimated by the algorithms were very stable on a day-to-day basis if those biases were derived from satisfactory solutions; that is, ones with high quality figures. Furthermore, in the case of single-pass determinations we found that the two biases, one corresponding to the solution on each side of the s/c sub-track, could be used to resolve the position ambiguity with respect to the sub-track. In fact, a subjective assessment indicated that a comparison of the biases was able to resolve the ambiguity better than a comparison of the quality figures. These statements are supported by material given in the next section -- at this point we note that a combined assessment of the accuracy of a two-pass position/velocity determination is available from the quality figure and the difference in estimated oscillator biases. The selection of a quality figure of 25 or less as indicative of an unsatisfactory fit is consistent with our assessment of the performance of the algorithm.

2.3 To demonstrate the stability of the oscillator biases estimated by the position-velocity algorithm we have tabulated data from three TWERLE platforms selected at random (except that one each was selected from the Ascension, Samoa, and Christchurch launches). The data tabulated in the Appendix shows the following: a) When high quality two-pass solutions indicated by quality figures greater than 30 and bias differences less than 50 hertz are considered the oscillator bias is conservative from day-to-day and week-to-week. Interdiurnal changes are typically a few to 10s of hertz whereas over a week the changes may be on the order of 50 hertz. b) Inclusion of bias estimates from high quality single pass solutions (quality figure >40) supports the above conclusion. c) In a significant fraction of the cases (8 out of 11) the selection of the ambiguous position with respect to the s/c subtrack on the basis of the oscillator bias nearest to the conservative previous value would have been correct, whilst the selection on the basis of the highest quality figure would have been wrong or inconclusive (quality figures equal). In these cases the 'correct' side was chosen by

reconstruction of the balloon trajectory in time. d) In three cases the resolution of ambiguous position on the basis of the oscillator bias fails. These cases are all apparently near the s/c subtrack and in one of these the quality figures were equal for the solution on each side.

2.4 The incorporation of the bias information into the position-velocity algorithm requires carrying that information from day to day. We suggest that a weighted running average of the bias information for the satisfactory location determinations be calculated and stored for each platform for use in the next position/velocity determination.

There are various choices and we suggest a simple one.

A. Define quantity POBIAS which is a weighted time-averaged quantity determined for each platform according to the following procedure:

1. Single Pass.

   If either quality figure is greater than 40, then choose the lesser of |BIAS1-POBIAS| and |BIAS2-POBIAS| = BIASX and POBIAS = (POBIAS+BIASX)/2. If not, POBIAS = POBIAS.

2. Two-pass.

   If |BIAS1-BIAS2| is less than 40 then POBIAS = (POBIAS+BIAS1+BIAS2)/3. If not, POBIAS = POBIAS.

B. Store new value of POBIAS for next 'day'.

C. Set 1st guess value of BIAS1 and BIAS2 = POBIAS in the position/velocity algorithm.

Various alternatives are possible. For example, the inflection point determined by the curve-fitting routine can be compared with POBIAS. If the difference exceeds 40-50 hertz then use POBIAS as the inflection point.

Figure 1 shows a plot of the bias data for two of the platforms together with POBIAS calculated from the above procedure.

3.0 Results of investigation of velocities derived from two single pass cases.

3.1 As a result of investigations into the performance of the position/velocity algorithm, Nimbus Operations instituted (during

early August) a revised procedure for processing two-pass data. If the quality figure was below 25, the two passes were split into two single-pass cases. Such action was justified because a) the low quality figure suggested that the great-circle-motion model assumed by the algorithm could not do a reasonable job of fitting the observed Doppler and b) the oscillator biases in these cases were frequently hundreds of hertz apart (see previous section). c) The velocities in almost all of these cases were unrealistic (e.g., speeds of hundreds of meters per second) and the positions did not correspond to those determined from single-pass cases for inclusive orbits. However, it was not clear that the velocities obtained by differencing the resulting two single-pass locations would be an adequate approximation to the velocity of the platform had the algorithm given a good solution. Obviously the only way to check this was to consider good two-pass cases (quality figure >25 and oscillation bias difference <40 hertz) and to split these into two single-pass cases for position differencing. Al Clark of Nimbus Operations performed these calculations for us using data on orbits 1410-1421 (days 268-269).

3.2 It is important for the reader to recall that the position velocity algorithm developed for TWERLE was based on the simultaneous solution of Doppler data from two passes assuming a model of platform motion along a great circle during the time interval between 1st contact of pass A to last contact on pass B. In particular, it seems always necessary to emphasize that the platform velocity is not calculated by locating the platform on successive plasses and then differencing these positions to obtain displacement (=velocity) vectors. However, it is of interest to know how well the algorithm would estimate platform motion if it were forced to operate in the latter mode. From the twelve orbits of data available thirty cases were extracted in which two-pass velocities and velocities determined from two single-pass calculations were made on commensurate data. These cases were selected to include platform motion from various directions and with a wide range in speeds and high quality single-pass location determinations (quality figure >40). Vector rms differences were calculated: the mean north-south velocity component difference was +1.2 mps and the mean east-west component +0.7 mps. The standard vector deviation was 3.1 mps. One case, in which the east-west velocity component difference was 40 mps and the north-south component difference was 17 mps, was eliminated from the sample. The former value was five times the next largest difference and the latter about 3 times the next largest. No obvious characteristic of the two-pass of single-pass cases suggested that either was an unsatisfactory solution. Apparently an occasional solution will

depart radically from a 'good' solution. With a larger sample the mean component differences might be expected to approach zero unless a systematic error is involved in either the two-pass or single pass solutions.

3.3 In view of the comparison above and the apparent success in obtaining good velocity data by differencing single-pass cases we agree with the procedure of splitting poor two-pass cases into single-pass solutions. The reasonably good comparison above raises some interesting questions about the nature of the position/velocity solution with a random Doppler system. However, a thorough investigation of these questions cannot be carried out at this time.

END OF MEMO

PRJ/kmn

cc: TWERLE Team
A. Clark, GSFC
M. Desbois
T. Green, GE
N. Levanon
E. Lichfield
W. Massman, UWis
J. Morakis, GSFC
T. O'Neill, NASA Hdqs.
B. Palmer, GSFC
D. Reed, ORI
R. Shapiro, GSFC
J. Theon, GSFC

October 16, 1975

MEMORANDUM

TO: TWERLE Team

FROM: Paul Julian

The enlcosed material represents my efforts at evaluating the performance of the TWERLE system. The analysis depends upon rawinsonde data from Ascension (a GMD-4 transponder system, no aneroid element) and Pago Pago (a GMD-2, standard radiosonde). The conclusions that I draw from the data are fairly obvious -- they are intended to stimulate discussion and I am confident they will. The TWERLE data are taken from the HANDAR data reduced by our people in the field. Checks using data from first (launch) day Nimbus data indicates good agreement in all but a few cases. Some Nimbus data (in parentheses) has been used, if no HANDAR data were available.

A. Radio Altimeter. We were fortunate to have excellent FPS-16 radar track for a number of our Ascension balloons. The data are set out in Table 1. The radar averages were supplied by Bill Massman. L. Julian, on Ascension, also calculated averages from the radar printout and from the HANDAR record. These averages were from 6 to 10 values for each for the balloon at altitude but were not always simultaneous. Some idea of the variation in averages, Massman vs. L. Julian for radar and Nimbus overpass vs. L. Julian (HANDAR), can be obtained by comparing the relevant columns. A few anomalous values have been, charitably, questioned. My conclusion is that the radar and radio altimeter agree near perfectly in the mean. The standard error (rms) (~40 m) is possibly a little large, but given the non-simultaneity of some of the averages and the fact that the balloon does move in the vertical may account for this value. Three of the Ascension test flights, 1974, have also been included.

B. Temperature Sensor. Before discussing the temperature sensor, which will be compared with the radiosonde temperature, a brief review of the subject of geopotential height is in order. Radiosonde soundings relate pressure and temperature to dynamic height, Z, where

$$Z = \frac{1}{9.8}\int g(\lambda,\phi,z)\,dZ = \frac{\Phi}{9.8}$$

and the integration of the hydrostatic equation is done in geopotential, Φ

$$\frac{dP}{d\Phi} = -\rho\ .$$

Thus, since the radio altimeter gives us geometric altitude we must always compare quantities in the same 'height' units; either geometric or dynamic height. For both Samoa and Ascension, and at 14 km the following obtain (units of Z are gm, not grams but geopotential meters)

14000 m = 13943 gm
14000 gm = 14057 m.

The temperature comparison was accomplished by taking the 150 mb temperature, correcting from dynamic to geometric height and then adjusting the radiosonde temperature to the geometric height of the balloon using a lapse rate of 0.60°C/100 m. This lapse rate at 14 km is appropriate to both Samoa and Ascension and is very constant in time. For the Ascension launches, Table 2, a total of 55 cases were used. The mean difference was 1.2°C with the TWERLE sensor running colder than the radiosonde. The rms difference was 1.2°C. This mean difference agrees well with Lichfield's value of -1.4°C obtained in the Ascension 1974 tests.

A similar comparison for the Samoa flights, 52 cases, gives a mean difference of -1.0°C with a standard error of 1.23. Since the temperature elements on both radiosondes are virtually identical the agreement is to be expected. However, since the radiosonde people maintain that solar radiation effects on their thermistor is negigible, we ought to take a further look at this difference.

C. Dynamic height. Direct comparison of the pressure sensor with an independent pressure is impossible, obviously, so I have elected to compare 150 mb dynamic heights. At Ascension this quantity is determined by a measurement of <u>surface</u> pressure and continuous integration of the hydrostatic equation using the measured mean virtual temperature. On Samoa this quantity is determined by stepwise integration of the hydrostatic equation by incremental pressure layers, the latter determined by the radiosonde pressure device.

The Samoa data are considered first (Table 2). These data are stratified into two groups, the first covering the days 182 through 217. In the latter part of this period, Levanon noticed that the recalibration pressures were consistently below the original calibration pressures and the Schwein gage was sent to Samoa (after some struggle) to check the TI gage. It was found that the TI gage was 2.7 mb too low. Therefore for all flights in this sample the dynamic height of the 150 mb surface as measured by TWERLE was calculated by

$$Z(dm) = (p-150.0+2.7)\cdot 40+z-57$$

where z=radio altimeter geometric height and p in mb from the pressure sensor. The 40 m/mb assumes a nominal temperature of -70°C. For the

sample of 30 cases, days 182-217, the mean TWERLE minus radiosonde 150 mb dynamic height was -23 gm, with a standard error of 48 gm.

The second sample runs from day 218 through 266. With the exception of the interval day 232-240 incl. the differences are of the same magnitude as in the pre-day 218 sample. However, a noticeable anomaly occurs in the 232-240 interval with the 150 mb height differences running 60-100 gm positive. Clearly, some explanation for this anomaly must be made. As of the present, I am endeavoring to find out the sequence of events on Samoa in regards to the details of the pressure sensor calibration. My perusal of the data in the Table suggests the pressure readings are the nub of the problem.

The analysis of comparable data on Ascension is set out in Table 3 . The same procedure as above was carried out except that the same Schwein gage calibration was carried through the entire series (by the site calibration procedure). The immediate and striking result is noticed that from days 188-211 the difference in 150 mb dynamic heights is small (-7 gm), but that from day 212 on a large negative difference obtains (-68 gm). A plot of these differences gives graphic evidence of a discontinuity at day 211.

A reconstruction of events on Ascension is as follows. Until day 212 the pressure units were calibrated according to standard procedure with the TI gage used in such a manner that it remained overnight (or from one series of calibrations to the next) at ambient pressure. Starting on day 212 the calibrations were performed with the TI gage held constantly at near 150 mb. Moreover, during the first week or so of August all unflown pressure units were checked to determine their storage pressure. All units that had leaked to storage pressures greater than 250 mb were pumped back to about 100 mb.

As a result of the discontinuous comparison results and the differing calibration details, a test was performed at Ascension before the TI gage was dismantled and using three unflown pressure sensors. The following procedure was followed: on the first day (9 Sept) the sensors were calibrated using normal procedure and with the TI gage having been held at ~150 mb. After calibration the TI gage was returned to ambient pressure and on the second day it was pumped back to ~150 mb and the three sensors recalibrated. On the third day the three were recalibrated once more, the TI gage having remained at 150 mb overnight. The results are set out in Table 4 , together with all other calibrations of these three sensors.

Table 4

ID	Manufacturers calib	Calib 5 or 12 Aug	9 Sept	10 Sept	11 Sept
145	151.73	150.28	147.27	147.42	147.38
192	151.33	147.79	144.71	144.95	144.72
198	150.23	146.31	143.96	144.18	144.10

My conclusion from these results is that the manner in which the TI gage is used does not contribute significant uncertainty to the calibration results. However, these results, whatever the ultimate explanation of them might be, are sufficient to explain the kind of behavior evident in the TWERLE-radiosonde comparisons.

Note that since we are running about 1.2°C colder than the radiosonde that the negative height differences are, from a hydrostatic point of view qualitatively consistent. Quantitatively, we may make use of Lichfield's result that the two temperature sensors agree quite well at about the 300 mb level, and calculate that the 300-150 mb thickness will be overestimated by an equivalent 0.6°C mean temp. This translates to a dynamic height overestimate of 0.6x20gm=12gm. Thus even though the comparison is qualitatively consistent, a quantitative cut suggests that the observed difference in the dynamic heights cannot be accounted for by differences in observed temperature alone. This conclusion, however, is somewhat dependent upon resolving apparent questions about the pressure sensor calibration.

At this point in time, my inclination is to use the radiosonde data whenever available to recalibrate the pressure sensor. This could be done by making use of the radio altimeter and temperature data to position the balloon on the radiosonde pressure-height curve. However, I am willing to enter into discussions concerning not only the interpretation of the above data, but what might be done about it.

D. Position/velocity data. Calibration of the RAMS position determination by use of the reference platforms suggests that we don't have any worries here. The magnitude of the difference vector (RAMS position-known position) is running, according to C. Cote, less than 2.5 km, once obvious errors are eliminated. However, the combined position/velocity accuracy must be looked at. The easiest ground truth is, again, available from the Ascension and Samoa rawinsondes. A comparison of the wind velocity vectors here is not all that one could hope for because (a) the space-time location of each vector is different and (b) the averaging procedure is different. Rawinsonde winds involve a 4000 foot vertical average of an ascending balloon whereas TWERLE winds involve a 108 minute time average of a horizontally-moving balloon.

Nevertheless, a comparison of 22 cases on Ascension gave a mean vector difference of 1.5 m per sec with a standard vector deviation of 5.1 mps. Eleven cases on Samoa gave 1.3 mps and 3.9 mps respectively. I am quite impressed with these results considering the above.

We have about a dozen cases for which we can get a FPS-16 horizontal (PPI) track of the TWERLE balloon over roughly the same time interval it was transmitting to Nimbus 6. As soon as we can reduce these data we will have much better comparisons.

END OF MEMO

PJ/kmn

Table 1

RADAR VS. RADAR ALTIMETER

			Massman	Radar Time	# pts 30 sec rate	Satellite	Time
182	1/7	1140	14321	10:24-10:37	28	14236	11.1
188	7/7	1464	14170	11:35-12:05	62	14220	12.1
189	8/7	1762	14393	11:15-11:43	58	-----	
190	9/7	0062	14198	11:27-11:50	46	14217	12.4
191	10/7	0352	14229	11:54-12:17	44	14230	13.3
192	11/7	0640	14334	10:24-10:54	60	14320	12.4
195	14/7	0570	14291	10:21-10:45	49	14310	10.5
197	16/7	0232	14176	10:59-11:29	60	14186	12.5
199	18/7	1357	14250	12:33-13:03	60	14050	14.6
204	23/7	0173	14392	11:10-11:40	61	14329	12.6
205	24/7	0457	14360	10:45-11:03	37	14297	12.0
206	26/7	1021	14460	10:31-11:03	64	14392	11.3
211	30/7	1635	14193	11:38-12:17	79	14139	14.6
212	31/7	1356	(14264	15:30-15:58	57)	too late	
216	4/8	1360	14095	12:34-13:31	114	14097	12.8
227	15/8	0216	14323	11:55-12:25	64		
231	19/8	1373	14307	12:37-13:36	115	14235	14.1
237	25/8	0267	14243	12:42-13:34	105	14222	13.5
240	28/8	1521	14280	11:01-11:41	83	14220	11.3
TA		1406	14190			14200	
TA		1212	14185			14200	
TA		0524	14160			14150	

* Same averaging interval

ASCENSION I

# pts	Radar RA (m)	Handar	On site Radar Average	Radar RA (m)	Radar Massman Radar on site
14	85	-----	-----		
15	-50	14194	14196	+ 2	-26
		14381	14374	- 7	+19
15	no lock	14151	14203	+ 52	- 5
?	- 1	14211	14334?	+123	-105
15	+14	14328	14334	+ 6	0
6	-10	14301	14300	- 1	- 9
15	-10	14194	14188	- 6	-12
15	no lock	no lock	14263	----	-13
15	+63	14325	14362	+ 37	+30
15	+63	14310	14374	+ 64	-14
15	+68	14398	14442	+ 44	+18
15	+54	14151	14204	+ 53	-11
		-----	14262	----	(+2)
13	- 2	14099	14102	+ 3	- 7
		14278	14348	+ 70	-25
10	+72	14231	14279	+ 48	+28
15	+21	14247*	14257*	+ 10	-14
15	+60	14229*	14297*	+ 68	-17

-10
-15
+10

Mean 23.7
S_x 40.3
$S_{\bar{x}}$ 9.8

Table 2
Samoa

	Date	ID	RA	T	P	150 mb Z	Tw-Raob (gm)	$Raob_Z$
182	1/7	1101	14385	71.8	143.0	14156	-14	14170
183	2/7	1137	14213	69.0	147.5	14156	+22	14134
183	2/7	1207	14280	68.6	144.4	14107	-27	14134
185	4/7	0023	14400	73.4	142.4	14147	-13	14160
189	8/7	0507	14321	67.4	143.8	14124	- 8	14132
190	9/7	0175	14291	70.4	145.6	14166	- 3	14169
190	9/7	1643	14166	69.7	147.1	14101	-68	14169
(190)	9/7	0531	14245	68.4	147.1	14184	+15	14169
191	10/7	0467	14380	71.0	143.0	14151	-23	14174
192	11/7	0761	14280	----	144.6	14115	-55	14170
192	11/7	1715	14321	70.8	144.6	14156	-14	14170
195	14/7	0576	13905	62.1	153.0	14076	-29	14105
(195)	14/7	0601	13782	61.4	155.4	14049	-56	14105
196	15/7	1316	14087	----	-----			
196	15/7	1351	14233	67.1	145.0	14084	- 5	14089
197	16/7	1320	14234	70.9	146.6	14149	-29	14178
198	17/7	1604	14205	69.0	146.8	14128	+28	14100
201	20/7	1632	14242	68.9	144.7	14081	-33	14114
201	20/7	0104	14321	69.3	142.5	14072	-42	14114
202	21/7	0202	14294	70.5	144.3	14117	-43	14160
202	21/7	0234	14262	68.9	145.2	14121	-39	14160
203	22/7	0416	14289	70.8	148.9?	14296	+106?	14190
203	22/7	1060	14439	70.7	-----			14190
205	24/7	1366	14403	71.4	141.8	14126	-26	14152
205	24/7	1572	14383	71.0	142.1	14118	-34	14152
(205)	24/7	1674	14418	71.1	140.2	14077	-75	14152
(205)	24/7	0142	14384	70.3	141.9	14111	-41	14152
211	30/7	0244	14096	69.4	148.3	14079	-91	14170
211	30/7	0450	14241	71.4	143.6?	14036	-134?	14170
212	31/7	0756	14271	70.7	145.3	14134	-16	14150
217	5/8	1317	14033	68.0	154.9?	14280	+101?	14179
217	5/8	1535	14224	68.0	146.3	14127	-52	14179
						mean	-23.3	
						S_x	47.6	
						$S_{\bar{x}}$	8.7	

$Raob_T$	z=Z+57	AdjT	Tw_T-RS_T
69.1	14227	70.1	-1.7
68.1	14197	68.2	0.8
68.1	14197	68.6	0
69.3	14217	70.5	-2.8
68.6	14189	69.4	-2.0
68.7	14226	69.1	-1.3
68.7	14226	68.3	-1.4
68.7	14226	68.8	+0.4
68.8	14231	69.7	-1.3
67.9	14207	----	
67.9	14207	68.6	-2.2
61.7?	14162	----	
61.7?	14162	----	
66.1	14146	66.6	-0.5
67.1	14235	67.1	-3.8
69.1	14157	69.4	+0.4
67.1	14171	67.5	-1.4
67.1	14171	68.0	-1.3
69.5	14217	70.0	-0.5
69.5	14217	69.8	+0.9
68.1	14247	68.3	-2.5
68.1	14247	68.8	-1.9
69.5	14209	70.7	-0.7
69.5	14209	70.5	-0.6
69.5	14209	70.8	-0.3
69.5	14209	70.5	+0.2
68.7	14227	67.9	-1.5
68.7	14227	68.8	-2.6
68.7	14207	69.1	-1.8
68.0	14236	66.8	-1.2
68.0	14236	68.0	0

Samoa

	Date	ID	RA	T	P	150 Z (gm)
218	6/8	1633	14152	68.5	149.7	14083
227	15/8	0311	14300	69.0	145.9	14079
227	15/8	0327	14330	70.1	144.9	14069
232	20/8	0360	14195	67.1	152.7	14246
232	20/8	0505	14170	----	153.7	14261
232	20/8	0372	14233	64.4	150.5	14196
233	21/8	0017	14220	67.5	153.5	14303
233	21/8	0452	14137	66.0	154.8	14272
234	22/8	0517	14188	67.7	154.0	14291
234	22/8	0533	14175	68.7	154.9	14314
234	22/8	0574	14262	68.6	151.1	14249
237	25/8	0627	14090	68.7	155.4	14249
237	25/8	0644	14274	69.1	150.8	14249
238 (239)	26-7/8	0656	14175	72.5?	154.4	14294
238 (239)	26-7/8	0542	14239	69.1	153.4	14318
239 (240)	27-8/8	0566	14172	----	151.2	14163
239 (240)	27-8/8	0660	14199	66.5	153.6	14286
239 (240)	27-8/8	0672	14050	66.3	156.6	14257
240	28/8	0762	14138	60.9?	155.3	14293
240	28/8	0754	13991	?	155.7	14162
241	29/8	1013	14076	65.4	153.9	14175
241	29/8	1127	14205	66.5	150.4	14164
244	1/9	1135	14300	68.8	146.4	14099
244	1/9	1274	14309	69.3	146.8	14124
259	16/9	1025	14294	67.3	148.6	14185
260	17/9	1455	14225	66.8	148.8	14120
261	18/9	1765	14133	67.2	151.4	14132
261	18/9	0550	14256	70.9	148.1	14123
262	19/9	0324	14233	67.2	147.3	14068
265	22/9	0636	14036	67.1	152.8	14091
266	23/9	0014	14196	66.4	148.4	14075

T_w-Raob (gm)	Raob Z	Raob T	z=Z+57	AdjT	$T_{Tw}-T_{RS}$
-151	14234	66.5	14291	67.7	-0.8
- 81	14160	68.7	14217	69.2	+0.2
- 91	14160	68.7	14217	----	
+76	14170	65.1	14227	64.9	-2.2
+ 91	14170	65.1		----	
+ 26	14170	65.1	14227	65.1	+0.7
+150	14153	65.6	14227	65.7	-1.8
+119	14153	65.6	14210	65.2	-0.8
+ 96	14195	67.2	14210	66.8	-0.9
+119	14195	67.2	14252	66.2	-2.5
+ 54	14195	67.2	14252	67.3	-1.3
+ 64	14185	67.3	14252	66.4	-2.3
+ 64	14185	67.3	14242	67.5	-1.6
+ 92	14202	64.7	14242	64.2	(-8.3)
+116	14202	64.7	14259	64.6	-4.5
- 18	14181	65.6	14238	----	
+105	14181	65.6	14238	65.4	-1.1
+ 76	14181	65.6	14238	64.5	-1.8
+133	14160	67.3	14217	66.8	(+5.9)
+ 2	14160	67.3	14217	----	
- 28	14203	66.3	14260	65.2	-0.2
- 39	14203	66.3	14260	66.0	-0.5
- 43	14142	66.9	14199	67.5	-1.3
- 18	14142	66.9	14199	67.5	-1.8
+ 5	14180	67.7	14237	68.0	+0.7
- 52	14172	67.3	14229	67.3	+0.5
- 13	14119	69.4	14176	69.2	+2.0
+ 4	14119	69.4	14126	69.9	-1.0
-112	14180	M	14237	----	
- 19	14110	67.5	14167	67.3	+0.2
- 55	14130	65.9	14207	65.8	-0.6

$\bar{x}$ -1.03

S_x 1.23

$S_{\bar{x}}$ 0.17

Table 3
Ascension

	Date	ID	RA(m)	T	P	150mbZ (gm)	Tw-Raob (gm)	Raob Z (gm)
188	7/7	1464	14194	71.0	150.1	14141	-9	14150
189	8/7	1762	14381	----	145.5	14144	+4	14140
190	9/7	1754	14325	----	145.5	14088	-42	14130
190	9/7	0062	14151	77.1?	150.7	14122	-8	
191	10/7	0352	14211	68.5	149.2	14122	-8	14130
191	10/7	0364	14307	70.0	146.4	14106	-24	
191	10/7	0546	14310	70.0	147.0	14133	+3	
192	11/7	0640	14328	70.1	146.6	14135	(+5)	14030?
192	11/7	0676	14257	68.7	(?)143.0*	(14138)*	(+8)	(14130)
195	14/7	0570	14301	72.3	147.0	14124	-26	14150
195	14/7	1310	14220	71.2	149.5	14143	-7	
195	14/7	1016	14257	71.1	148.6	14144	-6	
196	15/7	0134	14257	65.8	148.9	14156	-4	14160
197	16/7	0232	14194	65.7	150.3	14149	+9	14140
197	16/7	0720	14234	66.9	148.7	14125	-15	
199	18/7	1357	-----	69.6	148.2	-----		14130
199	18/7	1067	14348	70.4	146.3	14143	+12	
199	18/7	1361	14284	70.0	146.9	14103	-27	
202	21/7	1645	14354	68.9	145.5			MSNG
202	21/7	1543	14136	68.5	150.8			
204	23/7	0173	14325	73.4	145.4	14084	-36	14120
204	23/7	0275	14473	73.8	142.2	14104	-16	
204	23/7	0243	14503	74.8	142.2	14134	+14	
205	24/7	0457	14310	72.6	146.6	14117	-23	14140
205	24/7	0767	14386	?71.9*	145.7	14157	+17	
211	30/7	1635	14151	68.5	157.0(?)			14140
211	30/7	0103	14154	69.3	151.4	14153	+13	
211	30/7	0205	14313					

23	-7.2
S_x	16.7
$S_{\bar{x}}$	3.5

Raob T	z of T	Adj T	Tw -RS T T
68.5	14207	68.4	-2.6
69.1	14197	----	---
69.9	14187	----	---
		----	---
68.3	14187	68.5	0
		69.0	-1.0
		69.0	-1.0
70.3		---	---
		---	---
		70.3	-2.0
69.7	14207	69.8	-1.4
		70.0	-1.1
66.5	14217	66.8	+1.0
65.7	14197	65.7	0
		65.9	-1.0

67.3	14187	68.3	-2.1
		67.9	-2.1
day 203 14120 67.3			
		71.8	-1.6
70.9	14177	72.7	-1.1
		72.8	-2.0
70.1	14197	70.8	-1.8
		71.2	-0.7
		67.8	-0.7
68.1	14197	67.8	-1.5

	Date	ID	RA(m)	T	P	150mbZ (gm)
212	31/7	1050	14328	68.9	147.2	14159
212	31/7	1066	14177	69.0	150.5	14140
216	4/8	1360	14099	67.1	151.4	14098
216	4/8	1542	14434	69.3	143.2	14105
216	4/8	1574	14159	67.9	150.6?	14126
218	6/8	1644	14174	67.5	150.1	14121
218	6/8	0144	14214	67.4	148.2	14085
218	6/8	1672	14252	68.7	147.6	14099
219	7/8	0274	14278	67.9	-----	-----
219	7/8	0172	14228	66.1	148.1	14095
219	7/8	0242	14246	68.0	147.4	14085
220	8/8	0456	14220	70.6	147.1	14047
220	8/8	0460	14243	68.1	148.5	14126
220	8/8	0750	14470	70.4	141.8	14085
223	11/8	1302	14224	71.6	147.0	14047
224	12/8	1516	14154	69.1	(?)153.8*	(14115)*
224	12/8	1334	14307	71.5	146.2	14098

Tw-Raob (gm)	Raob Z (gm)	Raob T	z of T	Adj T	Tw_T-RS_T
-31	14190	65.3?	14247	----	
-50	14190	65.3?	14247	----	
-72	14170	67.3	14227	66.5	-0.6
-65	14170	67.3	14227	68.5	-0.8
-44	14170	67.3	14227	66.9	-1.0
-9	14130	66.1	14187	66.1	-1.4
-45	14130	66.1	14187	66.3	-1.1
-31	14130	66.1	14187	66.8	-1.9
	14200	65.7	14257	65.9	-2.0
-105	14200	65.7	14257	65.5	-0.6
-115	14200	65.7	14257	65.6	-2.4
-133	14180	66.3	14237	66.2	-4.4
-54	14180	66.3	14237	66.3	-1.8
-95	14180	66.3	14237	67.7	-2.7
-123	14170	69.7	14227	69.7	-1.9
-65	14180	67.5	14237	67.0	-1.9
-82	14180	67.5	14237	67.9	-3.6

	Date	ID	RA(m)	T	P	150mbZ (gm)	Tw-Raob (gm)	Raob Z (gm)
226	14/8	0126	14111	64.1	150.4	14070	-70	14140
226	14/8	0110	14119	64.4	150.8	14094	-46	14140
226	14/8	1610	14082	65.3	152.1	14109	-31	14140
227	15/8	0704	14226	65.3	148.6	14113	-87	14200
227	15/8	0216	14278	66.9	147.9	14137	-63	14200
230	18/8	1345	14068	65.8	151.8	14083	-97	14180
231	19/8	1373	14231	66.2	147.2	14062	-98	14160
233	21/8	1567	14207	68.7	149.2	14118		14290?
233	21/8	1661	14222	68.4	147.7	14073		14290?
234	22/8	0161	14321	69.2	145.9	14100	-80	14180
234	22/8	0157	14233	67.1	147.9	14092	-88	14180
234	22/8	1657	14306	67.9	148.9	14205	+25	14180
237	25/8	0267	14240		146.7	14051	-119	14170
237	25/8	0473	14252	69.0	147.3	14087	-83	14170
237	25/8	0251	14455	72.3	142.3	14090	-80	14170
238	26/8	0743	14202	69.3	148.3	14077	-83	14160
238	26/8	0775	14307	70.7	145.1	14054	-106	14160
239	27/8	1335	14292	69.2	147.5	14135	-25	14160
239	27/8	1033	14231	68.4	147.7	14082	-78	14160
240	28/8	1521	14231	68.3	148.3	14106	-44	14150
240	28/8	1627	14202	66.7	146.9	14021	-129	14150
241	29/8	0221	14105	66.9	152.3	14140	-30	14170
241	29/8	0127	14185	66.5	147.9	14044	-126	14170
244	1/9	0435	14366	70.5	148.3	14241	+81	14160
244	1/9	0403	14298	72.0	-----			14160

38

$T = -67.8$

$S_x = 43.7$

$S_{\bar{x}} = 7.1$

Raob T	z of T	Adj T	$Tw_T - RS_T$
66.5	14197	66.0	+1.9
66.5	14197	66.0	+2.1
66.5	14197	65.8	+0.3
66.1	14257	65.9	+0.6
66.1	14257	66.2	-0.7
66.3	14237	65.3	-0.5
66.3	14217	66.4	+0.2
63.9?	-----		
63.9?	-----		
66.3	14237	66.8	-2.4
66.3	14237	66.3	-0.8
66.3	14237	66.7	-1.2
67.5	14227		
67.5	14227	67.7	-1.3
67.5	14227	68.9	-3.4
68.9	14217	68.8	-0.5
68.9	14217	69.5	-1.2
67.1	14217	67.5	-1.7
67.1	14217	67.2	-1.2
68.9	14207	69.1	+0.8
68.9	14207	68.9	+2.2
65.3	14227	64.6	-2.3
65.3	14227	65.6	-0.9
70.3	14217	71.2	+0.7
70.3	14217		

55

$\bar{x} = -1.19$

$S_x = 1.24$

$S_{\bar{x}} = 0.17$